materials

MDPI

Supporting information

Heterocycle Effects on the Liquid Crystallinity of Terthiophene Analogues

David F. Ester [1], Declan McKearney [1], Khrystyna Herasymchuk [1] and Vance E. Williams [1,*]

[1] Department of Chemistry, Simon Fraser University, 8888 University Drive, Burnaby, BC V5A 1S6 Canada; vancew@sfu.ca

1. Synthesis and Identification

All solvents used were reagent grade. 1-Bromooctane was purchased from TCI America. Triethylamine was purchased from Anachemia. All other reagents were purchased from Sigma-Aldrich. All reagents were used as received without further purification. Column chromatography was performed on silica gel 60 (230-400 mesh) purchased from Silicyle Inc. $CDCl_3$ was obtained from Cambridge Isotope Laboratories Inc.

400 MHz ^{1}H NMR spectra were run on a Bruker AMX-400 400 MHz NMR spectrometer. 500 MHz ^{1}H NMR spectra were run on a Varian AS500 Unity Inova 500 MHz spectrometer. High resolution mass spectrometry was carried out on a Bruker micrOTOF II LC/MS (ESI^+) by Nonka Sevova at Notre Dame Mass Spectrometry and Proteomics facility.

The final target compounds were prepared according to the procedures described in the experimental section of the paper. The synthetic procedures for any precursors and literature compounds are outlined below. The percent yield and detailed ^{1}H and ^{13}C NMR and mass spec data for all compounds are given below.

1.1. Precursors and literature compounds

2-Decylthiophene: In an oven-dried 100 mL 3-neck round bottom flask, thiophene (1.0 g, 11.9 mmol) in dry THF was cooled to -78 °C under a nitrogen atmosphere. n-Butyllithium (0.95 eq., 2.5 M solution in hexanes) was added drop-wise. The mixture was stirred at 0 °C for 60 minutes. Once cooled back to -78 °C, 1-bromodecane (0.90 eq.) was added slowly. The reaction was allowed to warm to room temperature and stirred overnight. It was then quenched with water, extracted with diethyl ether (3x50 mL), and the combined organic fractions were dried over magnesium sulfate. The crude was purified by vacuum distillation to give the product as a yellow oil (81 % yield). ^{1}H NMR (500 MHz, Chloroform-*d*) δ 7.18 (dd, *J* = 5.1, 1.1 Hz, 1H), 7.00 (dd, *J* = 5.1, 3.4 Hz, 1H), 6.87 (d, *J* = 3.2 Hz, 1H), 2.93 (t, *J* = 7.7 Hz, 2H), 1.79 (p, *J* = 7.4 Hz, 2H), 1.53 – 1.33 (m, 16H), 1.02 (t, *J* = 6.8 Hz, 3H) ppm.

5-Decyl-2-thiophenecarboxylic acid: In an oven-dried 100 mL 3-neck round bottom flask, 2-decylthiophene (1.0 g, 4.46 mmol) in dry diethyl ether was cooled to -78 °C under a nitrogen atmosphere. n-Butyllithium (1.2 eq., 2.5 M solution in hexanes) was added drop-wise. The mixture was stirred at 0 °C for 60 minutes. Once cooled back to -78 °C, carbon dioxide (excess) in the form of dry ice chunks was added. The reaction was allowed to warm to room temperature and stirred overnight. The precipitate was filtered and washed with diethyl ether then 10% hydrochloric acid and dried under high vacuum overnight to give the product as a white solid (69 % yield). ^{1}H NMR (500 MHz, Chloroform-*d*) δ 7.70 (d, *J* = 3.6 Hz, 1H), 6.80 (d, *J* = 3.5 Hz, 1H), 4.65 (s, 1H), 2.83 (t, *J* = 7.6 Hz, 2H), 1.69 (p, *J* = 7.5 Hz, 2H), 1.43 – 1.18 (m, 15H), 0.88 (t, *J* = 6.8 Hz, 3H) ppm.

Hydrazide derivative **1**: In an oven-dried 25 mL 3-neck round bottom flask, 5-decyl-2-thiophenecarboxylic acid (1.0 g, 3.52 mmol) was refluxed in thionyl chloride (5 mL, excess) under a nitrogen atmosphere for 2 hours. After cooling to room temperature, remaining thionyl chloride was removed via high vacuum overnight to generate 5-decyl-2-thiophenecarbonyl chloride in situ. This –oyl chloride was added to an oven-dried 50 mL 3-neck round bottom flask containing dry NMP. Triethylamine (3 mL, excess) was added followed by the drop-wise addition of hydrazine hydrate (0.7 eq.) at 0 °C. The mixture was warmed to room temperature and stirred overnight. The resulting

precipitate was collected by filtration. This crude product was purified by column chromatography on silica treated with 2% trimethylamine using a gradient from 0 to 50 % of ethyl acetate in hexanes as the eluent. The pure product was isolated as a white powder (37 % yield). ^{1}H NMR (500 MHz, Chloroform-*d*) δ 9.04 (s, 2H), 7.52 (d, *J* = 3.7 Hz, 2H), 6.76 (d, *J* = 3.7 Hz, 2H), 2.81 (t, *J* = 7.6 Hz, 4H), 1.67 (p, *J* = 7.5 Hz, 4H), 1.26 (s, 28H), 0.88 (t, *J* = 6.9 Hz, 6H) ppm.

α-Terthienyl, **Th$_3$**: Magnesium turnings (0.90 g, 37.0 mmol) were added to a 100 mL 3-neck round bottom flask, which was then sealed, purged with N_2, and flame dried. Added dry diethyl ether (50 mL) and cooled to 0 °C, followed by slow addition of 2-bromothiophene (3.26 mL, 33.7 mmol). Solution was warmed to room temperature and then refluxed for 2 hours to generate the Grignard solution. An oven-dried 250 mL 3-neck round bottom flask was charged with [1,3-bis(diphenylphosphino)propane] dichloronickel(II) (catalytic, ~2%) and cycled between N_2 and vacuum three times. Dry diethyl ether (150 mL) and then 2,5-dibromothiophene (1.71 mL, 15.3 mmol) were added and the solution was cooled to 0 °C. The Grignard solution prepared in situ was then added dropwise, the reaction was warmed to room temperature and then refluxed for 2 hours. After cooling to room temperature, the reaction was quenched by slow addition of 10% hydrochloric acid, the organic was separated out, and the aqueous was further extracted with diethyl ether (3x75 mL). The combined organic fractions were dried over magnesium sulfate. The crude was purified by column chromatography on silica using 5% ethyl acetate in hexanes as the eluent to give the final product (57 % yield). ^{1}H NMR (500 MHz, Chloroform-*d*) δ 7.23 (dd, *J* = 5.1, 1.2 Hz, 2H), 7.18 (dd, *J* = 3.6, 1.2 Hz, 2H), 7.09 (s, 2H), 7.03 (dd, *J* = 5.1, 3.6 Hz, 2H) ppm.

Th$_3$(10): A flame-dried 50 mL three-neck round bottom flask was charged with **Th$_3$** (0.15 g, 0.60 mmol) and cycled between high vacuum and N_2 atmosphere three times. Dry THF (25 mL) was added by cannula and the solution was cooled to around -78 °C prior to the drop-wise addition of n-butyllithium solution (2.5 M, 2.5 equivalents). After stirring for 30 minutes, potassium t-butoxide (1.0 M solution, 2.5 equivalents) was added and the solution was stirred for another 30 minutes. Then 1-decylbromide (2.2 equivalents) was added drop-wise. This mixture was warmed to room temperature and stirred overnight. The reaction was quenched with water (40 mL) and extracted with hexanes (3x30 mL). The combined organic fractions were dried over magnesium sulfate. Further purification was done by column chromatography on silica using hexanes as the eluent. Recrystallization from ethanol afforded the product as a light yellow solid (49 % yield). ^{1}H NMR (500 MHz, Chloroform-*d*) δ 6.96 (t, *J* = 3.3 Hz, 4H), 6.67 (d, *J* = 3.4 Hz, 2H), 2.78 (t, *J* = 7.6 Hz, 4H), 1.67 (p, *J* = 7.4 Hz, 4H), 1.42 – 1.21 (m, 28H), 0.92 – 0.84 (m, 6H) ppm. ^{13}C NMR (101 MHz, Chloroform-*d*) δ 145.56, 136.29, 134.79, 124.92, 123.60, 123.31, 32.06, 31.76, 30.35, 29.76, 29.71, 29.52, 29.48, 29.24, 22.84, 14.27 ppm.

Th-Thd-Th *core*: In a 150 mL high pressure vessel, 2-thiophenecarboxaldehyde (1.5 g, 13.4 mmol), sulfur (1.5 equivalents), and hydrazine hydrate (4.0 equivalents) were combined in propanol (10 mL). The mixture was allowed to react for 4 hours at 150 °C under high pressure. Once cooled to room temperature, the precipitate was collected by vacuum filtration. The crude was then dissolved in dichloromethane (150 mL), washed with saturated sodium sulfide (2x120 mL), water (1x150 mL), and then dried over magnesium sulfate. Recrystallization from ethanol afforded the final product as a light orange solid (88 % yield). ^{1}H NMR (500 MHz, Chloroform-*d*) δ 7.56 (dd, *J* = 3.7, 1.1 Hz, 2H), 7.50 (dd, *J* = 5.1, 1.1 Hz, 2H), 7.13 (dd, *J* = 5.0, 3.7 Hz, 2H) ppm. ^{13}C NMR (126 MHz, Chloroform-*d*) δ 161.18, 132.35, 129.65, 129.55, 128.14 ppm.

1.2. Oxadiazole derivative

Th-Oxd-Th(10): 64% yield. ^{1}H NMR (500 MHz, Chloroform-*d*) δ 7.60 (d, *J* = 3.7 Hz, 2H), 6.84 (dd, *J* = 3.7, 1.0 Hz, 2H), 2.87 (t, *J* = 7.6 Hz, 4H), 1.72 (p, *J* = 7.6 Hz, 4H), 1.42 – 1.23 (m, 30H), 0.88 (t, *J* = 6.9 Hz, 6H) ppm. ^{13}C NMR (126 MHz, Chloroform-*d*) δ 160.25, 151.93, 129.83, 125.48, 122.39, 32.04, 31.61, 30.40, 29.72, 29.67, 29.46, 29.17, 22.83, 14.27 ppm. HRMS (ESI$^+$ of m + H$^+$): m/z calcd for $C_{30}H_{47}N_2OS_2$: 515.3085, found: 515.3124.

1.3. Thiadiazole derivatives

Th-Thd-Th(4): 62% yield. ^{1}H NMR (500 MHz, Chloroform-*d*) δ 7.35 (d, *J* = 3.7 Hz, 2H), 6.79 (dd, *J* = 3.7, 1.0 Hz, 2H), 2.89 – 2.81 (m, 4H), 1.75 – 1.66 (m, 4H), 1.48 – 1.36 (m, 4H), 0.95 (t, *J* = 7.4 Hz, 6H) ppm. ^{13}C NMR (126 MHz, Chloroform-*d*) δ 160.96, 150.97, 129.74, 129.53, 125.30, 33.68, 30.15, 22.28,13.96 ppm. HRMS (ESI^{+} of m + H^{+}): m/z calcd for $C_{18}H_{23}N_2S_3$: 363.0979, found: 363.1018.

Th-Thd-Th(6): 29% yield. ^{1}H NMR (500 MHz, Chloroform-*d*) δ 7.35 (d, *J* = 3.7 Hz, 2H), 6.79 (dd, *J* = 3.7, 1.0 Hz, 2H), 2.85 (t, *J* = 7.6 Hz, 4H), 1.71 (p, *J* = 7.6 Hz, 4H), 1.43 – 1.29 (m, 12H), 0.92 – 0.87 (m, 6H) ppm. ^{13}C NMR (126 MHz, Chloroform-*d*) δ 160.97, 151.04, 129.73, 129.54, 125.29, 31.57, 30.47, 28.86, 22.70, 14.24, 14.19 ppm. HRMS (ESI^{+} of m + H^{+}): m/z calcd for $C_{22}H_{31}N_2S_3$: 419.1605, found: 419.1644.

Th-Thd-Th(8): 30% yield. ^{1}H NMR (500 MHz, Chloroform-*d*) δ 7.35 (d, *J* = 3.7 Hz, 2H), 6.79 (d, *J* = 3.7 Hz, 2H), 2.84 (t, *J* = 7.6 Hz, 4H), 1.71 (p, *J* = 7.6 Hz, 4H), 1.43 – 1.21 (m, 20H), 0.88 (t, *J* = 6.9 Hz, 6H) ppm. ^{13}C NMR (126 MHz, Chloroform-*d*) δ 160.97, 151.03, 129.73, 129.52, 125.28, 31.98, 31.61, 30.46, 29.37, 29.20, 22.80, 14.27, 14.23 ppm. HRMS (ESI^{+} of m + H^{+}): m/z calcd for $C_{26}H_{39}N_2S_3$: 475.2231, found: 475.2270.

Th-Thd-Th(10): 51% yield. ^{1}H NMR (500 MHz, Chloroform-*d*) δ 7.35 (d, *J* = 3.7 Hz, 2H), 6.79 (d, *J* = 3.7 Hz, 2H), 2.84 (t, *J* = 7.6 Hz, 4H), 1.71 (p, *J* = 7.5 Hz, 4H), 1.43 – 1.22 (m, 28H), 0.88 (t, *J* = 6.9 Hz, 6H) ppm. ^{13}C NMR (126 MHz, Chloroform-*d*) δ 160.97, 151.04, 129.74, 129.52, 125.29, 32.05, 31.61, 30.48, 29.73, 29.68, 29.47, 29.20, 22.84, 14.27 ppm. HRMS (ESI^{+} of m + H^{+}): m/z calcd for $C_{30}H_{47}N_2S_3$: 531.2857, found: 531.2896.

Th-Thd-Th(12): 69% yield. ^{1}H NMR (500 MHz, Chloroform-*d*) δ 7.35 (d, *J* = 3.6 Hz, 2H), 6.79 (d, *J* = 3.7 Hz, 2H), 2.84 (t, *J* = 7.6 Hz, 4H), 1.71 (p, *J* = 7.6 Hz, 4H), 1.41 – 1.22 (m, 36H), 0.88 (t, *J* = 6.9 Hz, 6H) ppm. ^{13}C NMR (126 MHz, Chloroform-*d*) δ 160.96, 151.03, 129.74, 129.51, 125.29, 32.07, 31.61, 30.47, 29.78, 29.68, 29.50, 29.46, 29.48, 29.19, 22.85, 14.27 ppm. HRMS (ESI^{+} of m + H^{+}): m/z calcd for $C_{34}H_{55}N_2S_3$: 587.3483, found: 587.3522.

2. Polarized Optical Microscopy (POM)

Polarized optical microscopy was carried out using an Olympus BX50 microscope equipped with a Linkam LTS350 heating stage. All images shown are of a size of ca. 920 x 1400 μm.

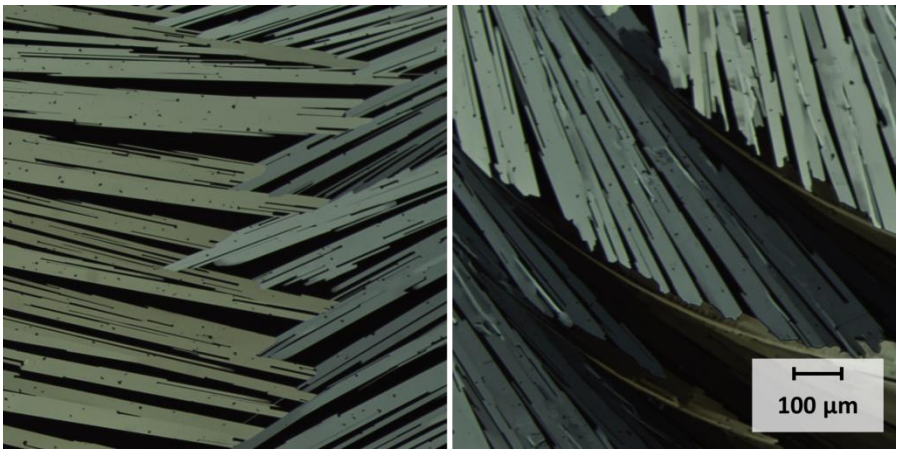

Figure S1. POM of **Th-Oxd-Th(10)** showing needle-like textures of the crystalline state at 72.0 °C.

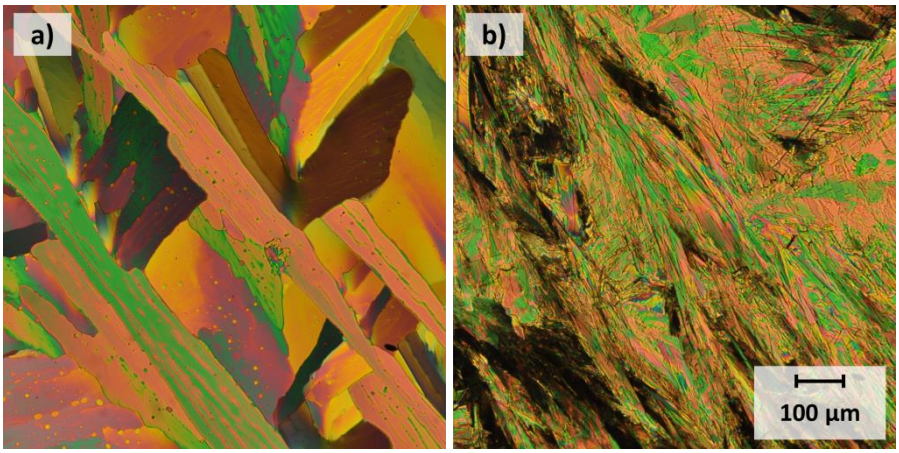

126

127 **Figure S2.** POM of **Th-Thd-Th(4)** showing needle-like textures of the crystalline state at 94.0 °C (a)
128 and at 25.0 °C (b).

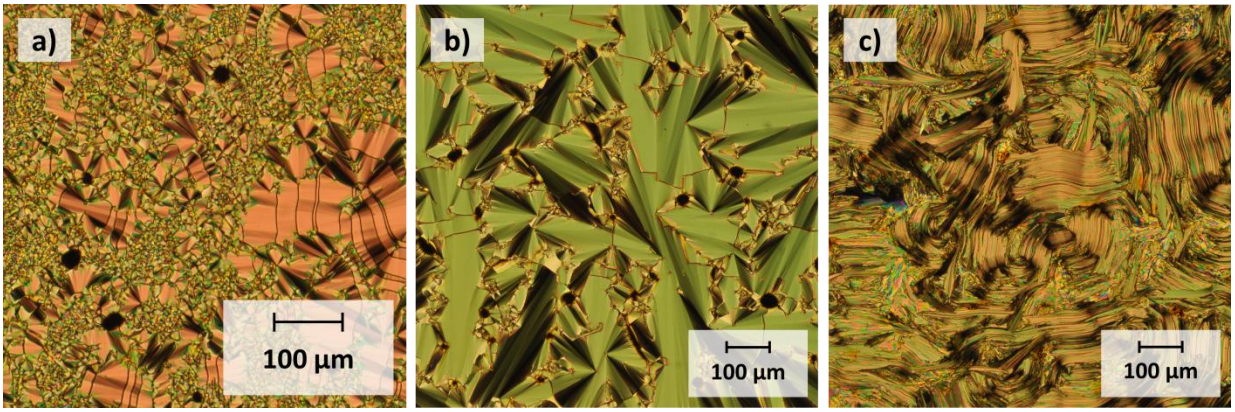

129

130 **Figure S3.** POM of **Th-Thd-Th(6)** showing schlieren and focal-conic textures of the SmC phase at
131 111.0 °C (a and b) and striations across focal-conic textures of the CrJ phase at 25.0 °C (c).

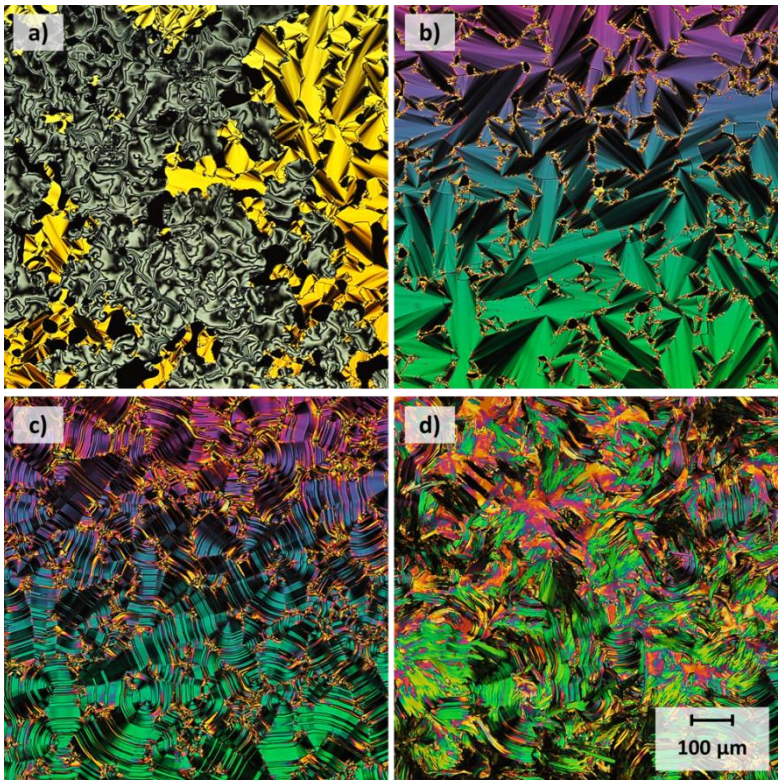

Figure S4. POM of **Th-Thd-Th(8)** showing schlieren and focal-conic textures of the SmC phase at 125.0 °C (a and b), striations across focal-conic textures of the CrJ phase at 88.0 °C (c), and changes upon cooling to the crystalline phase at 74.0 °C (d).

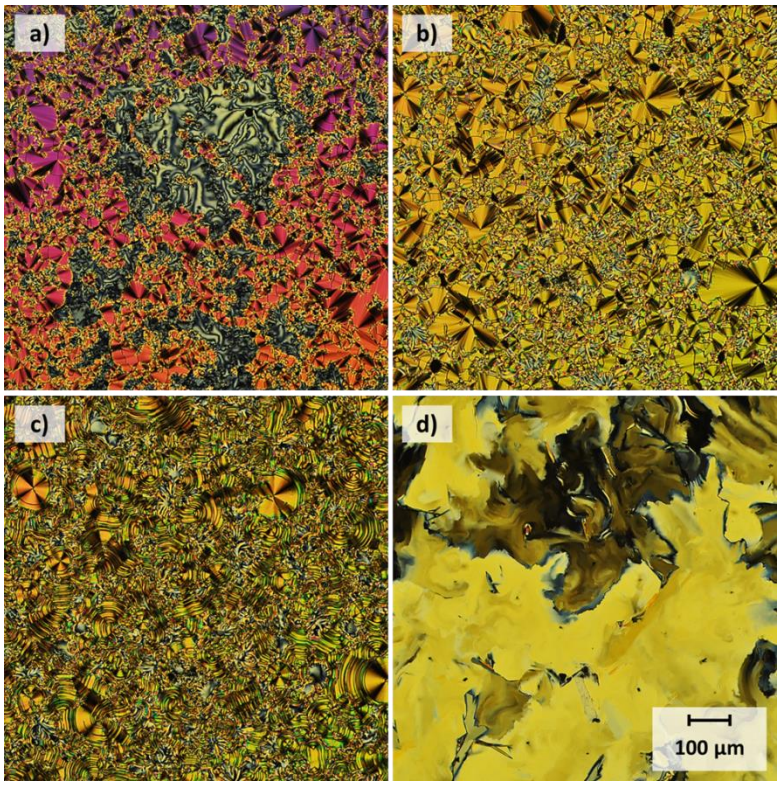

Figure S5. POM of **Th-Thd-Th(12)** showing schlieren and focal-conic textures of the SmC phase at 131.0 °C (a and b respectively), striations across focal-conic textures of the CrJ phase at 96.0 °C (c), and changes upon cooling to the crystalline phase at 87.0 °C (d).

3. Variable Temperature Powder X-ray Diffraction (VT-XRD)

X-ray scattering experiments were conducted using a Rigaku R-Axis Rapid diffractometer equipped with an in-house built temperature controller. [1]

Table 1. XRD parameters of the phases of **Th$_3$(10)** and **Th-Thd-Th(n)** (n = 6,8,10,12).

Compound (molecular length[a], nm)	Temperature (°C)	Phase	Layer spacing[b] (nm)	Correlation length[c] (nm)	# of layers	Tilt angle, θ (°)[d]
Th$_3$(10) (3.91)	91	SmF	3.60	26	7	23
	25	Cr	3.85	27	8	10
Th-Thd-Th(6) (2.95)	110	SmC	2.26	31	13	40
	76	CrJ	2.28	36	16	39
	25	CrJ	2.17	38	17	43
Th-Thd-Th(8) (3.47)	124	SmC	2.65	25	9	40
	83	CrJ	2.93	31	11	32
	25	Cr	2.49	38	15	44
Th-Thd-Th(10) (4.00)	126	SmC	3.01	31	10	41
	88	CrJ	3.33	32	10	34
	25	Cr	3.10	34	11	39
Th-Thd-Th(12) (4.49)	127	SmC	3.38	29	9	41
	101	SmI	3.66	29	8	35
	95	CrJ	3.69	25	7	35
	25	Cr	3.38	29	9	41

[a]calculated by DFT using B3LYP/6-31G*; [b]determined based on d_{001} peak; [c]calculated using Debye-Scherrer equation applied to d_{001} peak; [d]calculated from molecular length and layer spacing

Table S2. XRD data of **Th$_3$(10)** and **Th-Thd-Th(n)** (n=6,8,10,12).

Compound (molecular length[a], Å)	Temperature (°C)	Phase	d-spacings (Å)	Miller indices (hkl)
Th$_3$(10) (39.1)	91	SmF	36.0	001
			4.37	110
	25	Cr	38.5	001
			23.3	---
			19.6	002
			4.37	110
			3.78	---
			3.06	---
Th-Thd-Th(6) (29.5)	110	SmC	22.7	001
			4.37	alkyl halo
	76	CrJ	22.7	001
			11.4	002
			9.08	---

			7.22	003
			6.65	---
			6.24	---
			5.55	004
			4.82	---
			4.43	110
			3.62	---
			3.54	---
			3.27	---
			3.20	---
			21.7	001
			10.9	002
			7.12	003
			6.45	---
			5.78	---
	25	CrJ′	4.78	---
			4.34	110
			4.03	---
			3.55	---
			3.16	---
			3.02	---
	124	SmC	26.5	001
			4.37	alkyl halo
			29.3	001
			14.7	002
			9.83	003
			7.06	004
			6.73	---
			5.18	---
	83	CrJ	4.87	---
			4.45	110
			4.29	---
Th-Thd-Th(8) (34.7)			4.11	---
			3.81	---
			3.58	---
			3.30	---
			24.9	001
			12.5	002
			8.79	003
	25	Cr	5.78	---
			4.75	---
			4.32	110
			4.15	---

			3.54	---
			3.29	---
			3.14	---
Th-Thd-Th(10) (40.0)	126	SmC	30.1	001
			15.1	002
			4.37	alkyl halo
	88	CrJ	33.3	001
			16.7	002
			11.1	003
			9.94	---
			8.84	---
			7.59	---
			5.16	---
			4.29	110
			4.27	---
			4.07	---
			3.98	---
			3.80	---
	25	Cr	31.0	001
			15.4	002
			9.78	003
			7.25	---
			6.36	---
			5.04	---
			4.31	---
			4.22	110
			4.11	---
			3.94	---
			3.79	---
			3.65	---
			3.54	---
Th-Thd-Th(12) (44.9)	127	SmC	33.8	001
			17.1	002
			4.37	alkyl halo
	101	SmI	36.6	001
			18.5	002
			4.37	110
	95	CrJ	36.9	001
			18.8	002
			12.4	003
			9.98	---
			8.95	004

			5.13	---
			4.52	---
			4.33	110
			4.24	---
			4.02	---
			3.88	---
			3.74	---
			3.52	---
			33.8	001
			17.1	002
			11.8	003
			9.83	---
			8.61	004
			7.65	---
	25	Cr	5.07	---
			4.26	110
			4.17	---
			3.80	---
			3.67	---
			3.55	---
			3.44	---

[a]calculated by DFT using B3LYP/6-31G*

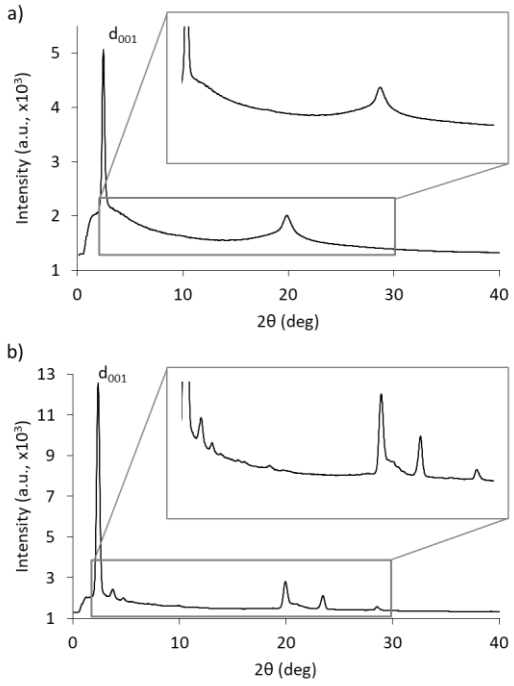

Figure S6. XRD of **Th₃(10)** at 91 °C, in the SmF phase (a) and at 25 °C, in the crystalline phase (b).

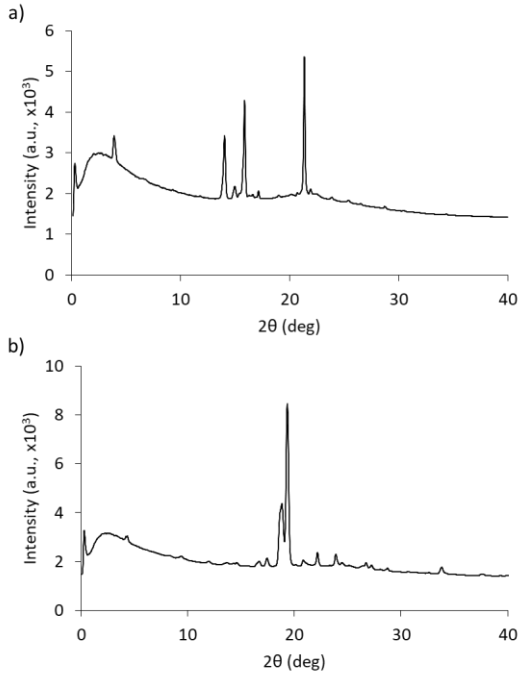

150

151 **Figure S7.** XRD of **Th-Oxd-Th(10)** at 70 °C, in the Cr phase (a) and at 25 °C, in the Cr″ phase (b).

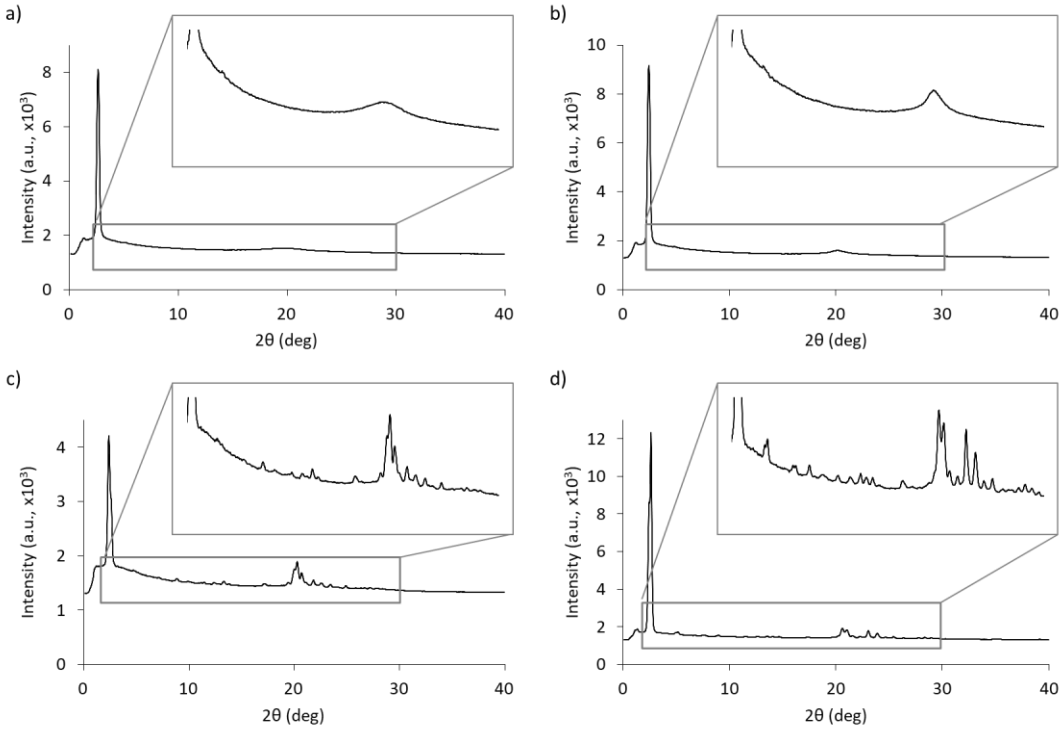

152

153 **Figure S8.** XRD of **Th-Thd-Th(12)** at 127 °C, in the SmC phase (a); at 101 °C, in the SmI phase (b); at
154 95 °C, in the CrJ phase (c); and at 25 °C, in the crystalline phase (d).

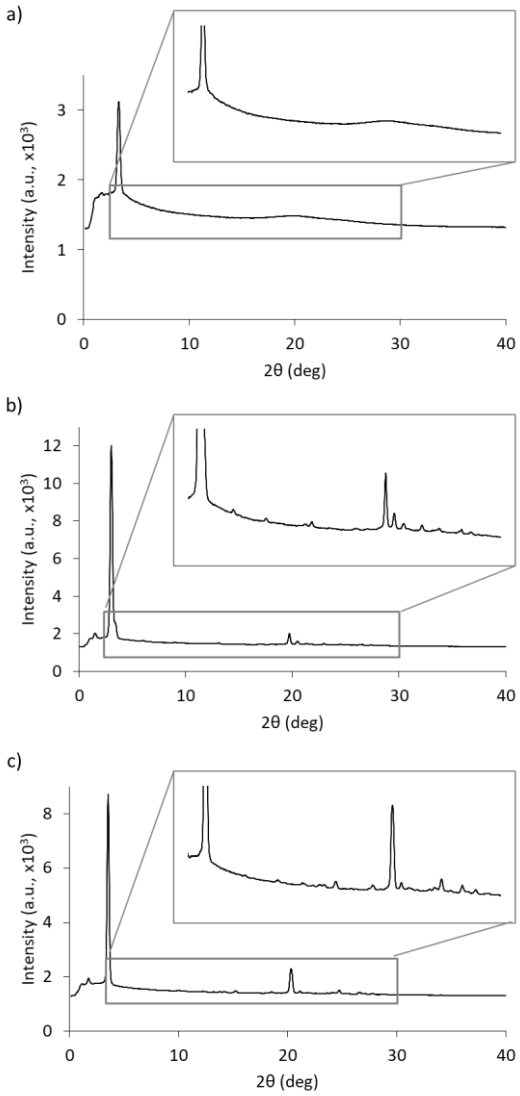

Figure S9. XRD of **Th-Thd-Th(8)** at 124 °C, in the SmC phase (a); at 83 °C, in the CrJ phase (b); and at 25 °C, in the crystalline phase (c).

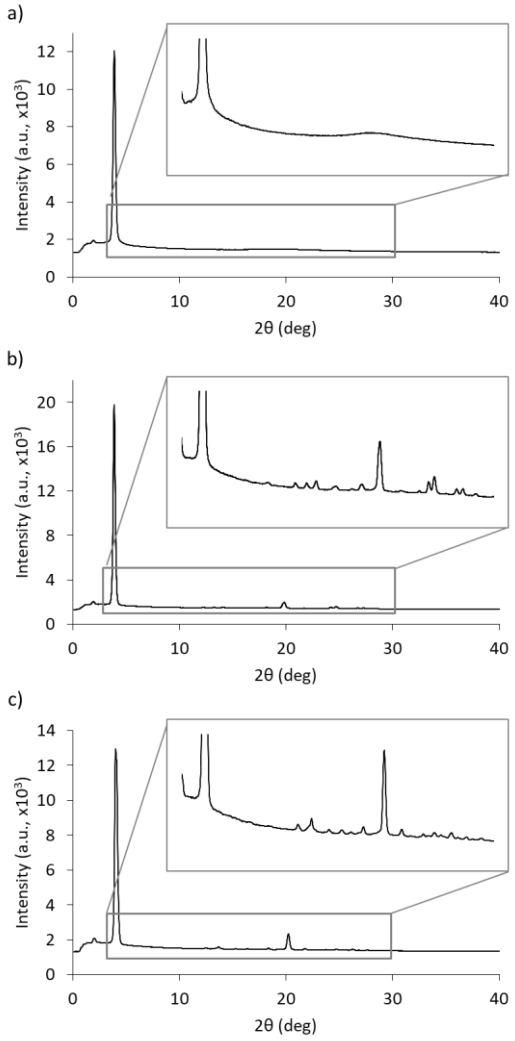

Figure S10. XRD of **Th-Thd-Th(6)** at 110 °C, in the SmC phase (a); at 76 °C, in the CrJ phase (b); and at 25 °C, in the crystalline phase (c).

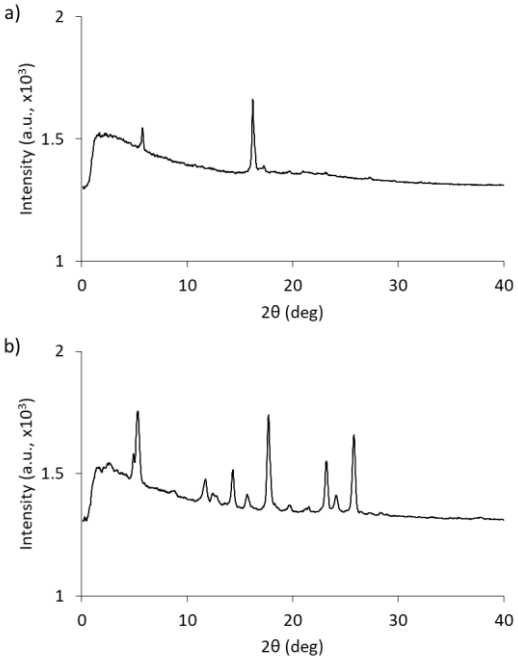

Figure S11. XRD of **Th-Thd-Th(4)** at 94 °C, in the Cr phase (a) and at 25 °C, in the Cr″ phase (b).

4. Differential Scanning Calorimetry (DSC)

Phase transition temperatures and enthalpies were determined using differential scanning calorimetry (DSC) on a TA Instruments DSC Q2000 equipped with a TA Instruments Refrigerated Cooling System 90, heating and cooling at a rate of 10°C min^{-1}.

Table S3. Phase transition temperatures and enthalpies of **Th_3(n)** reported by Boucher et al. [2].

n	Transition Temperature/ °C [enthalpy/ kJ mol^{-1}]
5	**Cr** 46 [15.2] **CrG** 76 [13.6] **I**
6	**Cr** 51 [16.7] **CrG** 81 [16.4] **I**
7	**Cr** 52 [17.8] **CrG** 75 [3.8] **SmF** 82 [0.7] **SmC** 86 [7] **I**
8	**Cr** 64 [24.4] **CrG** 71 [3.3] **SmF** 85 [1.6] **SmC** 90 [7.3] **I**
9	**Cr** 66 [30.8] **SmF** 91 [1.8] **SmC** 94 [10.4] **I**
10	**Cr1** 43 [2.3] **Cr2** 71 [32.1] **SmF** 92 [2.7] **SmC** 95 [10.5] **I**

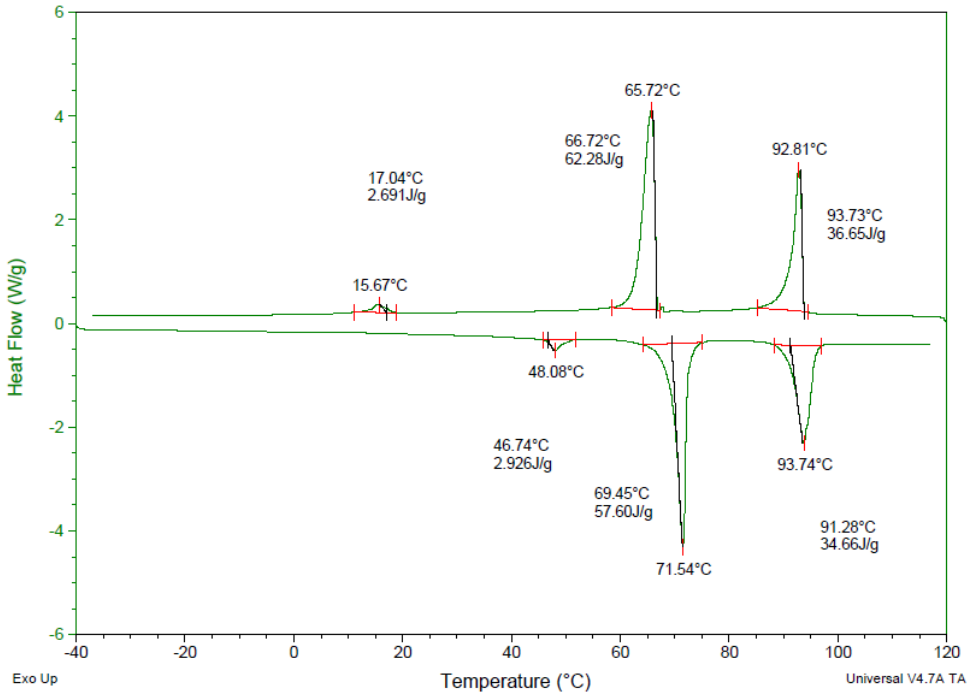

(a)

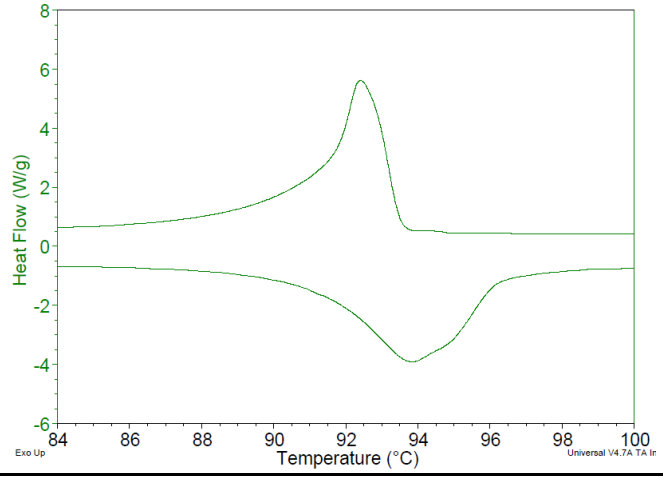

(b)

Figure S12. DSC thermogram of **Th$_3$(10)** (a), including zoomed in high temperature peak (b).

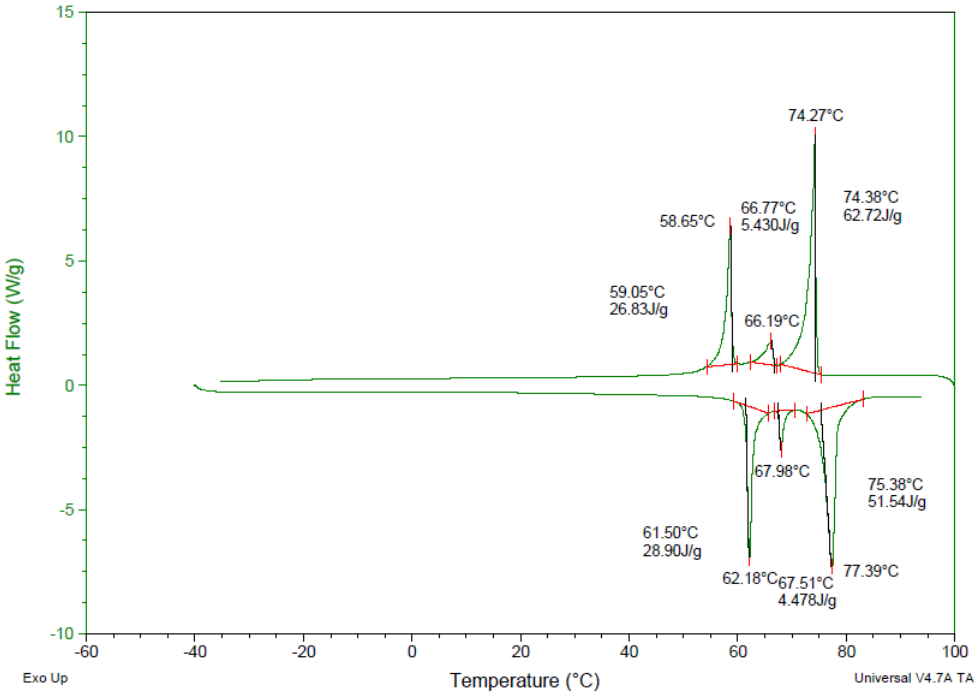

Figure S13. DSC thermogram of **Th-Oxd-Th(10)**.

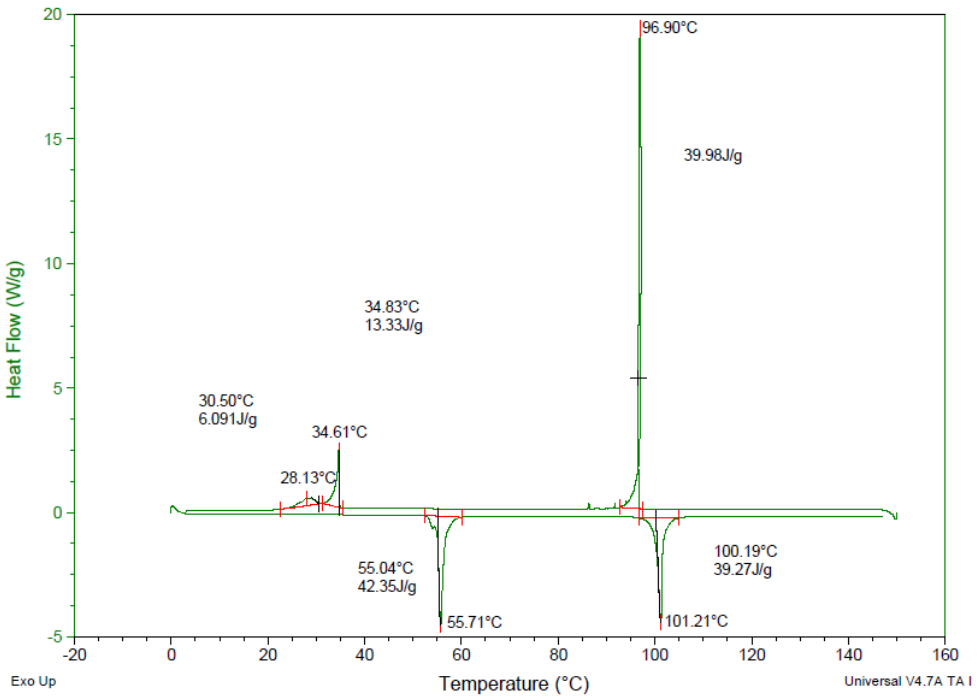

Figure S14. DSC thermogram of **Th-Thd-Th(4)**.

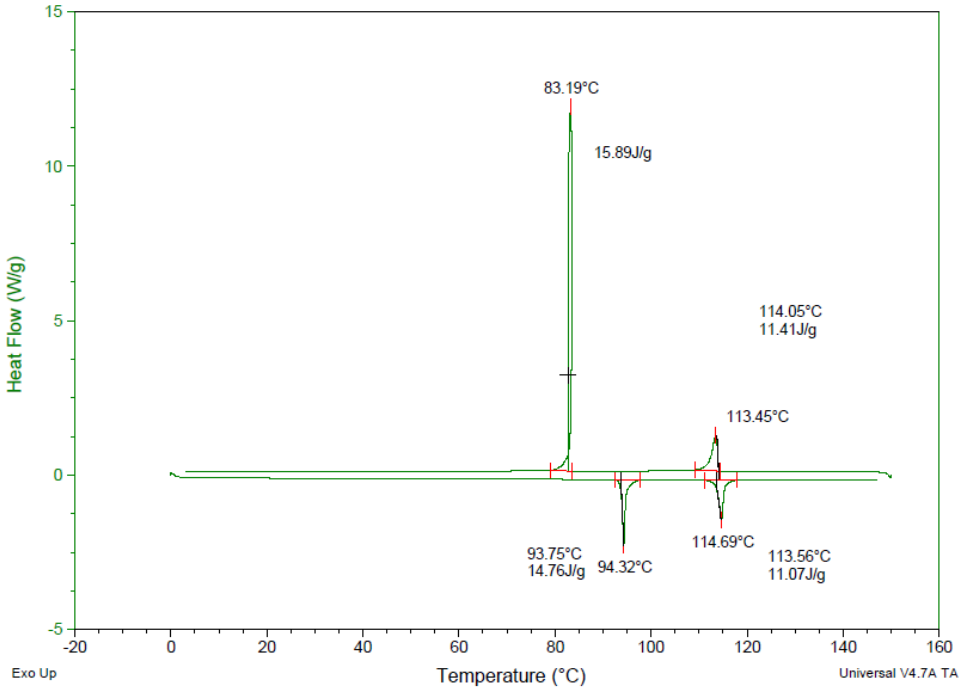

Figure S15. DSC thermogram of **Th-Thd-Th(6)**.

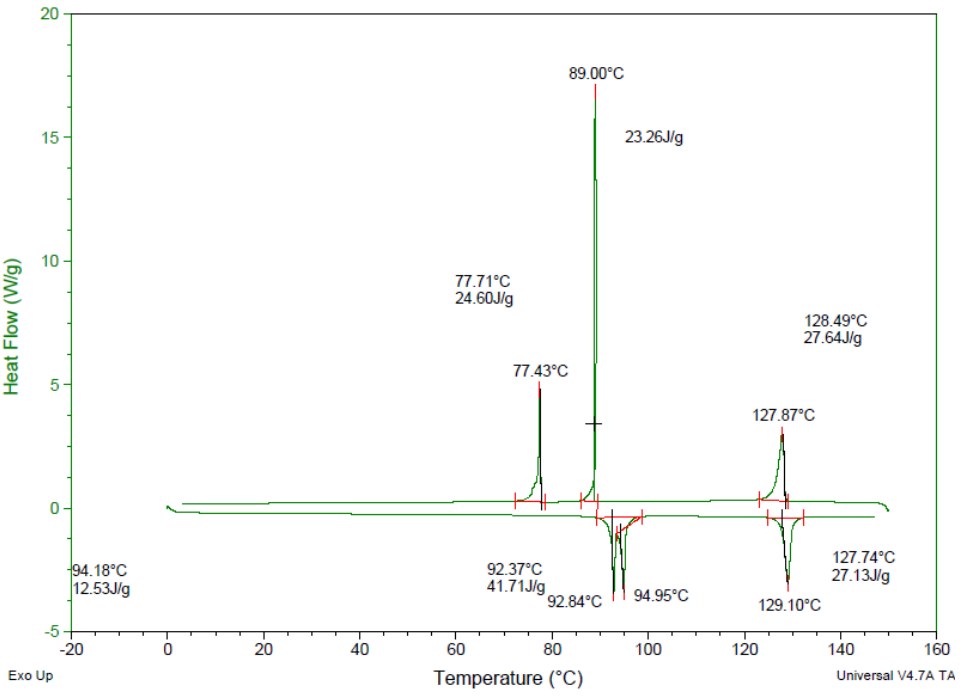

Figure S16. DSC thermogram of **Th-Thd-Th(8)**.

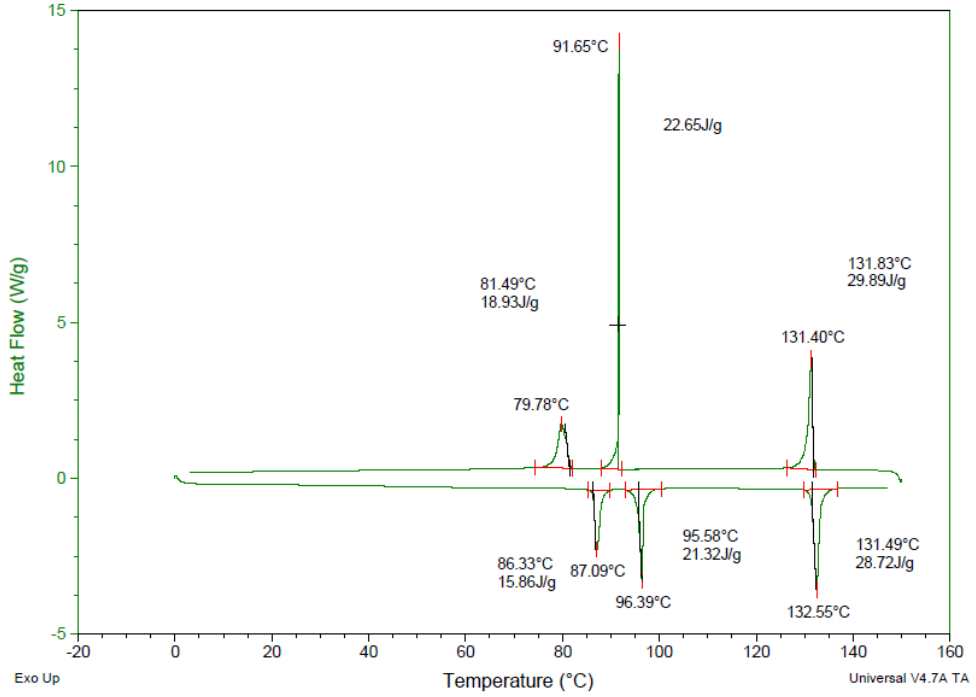

177

178 **Figure S17.** DSC thermogram of **Th-Thd-Th(10)**.

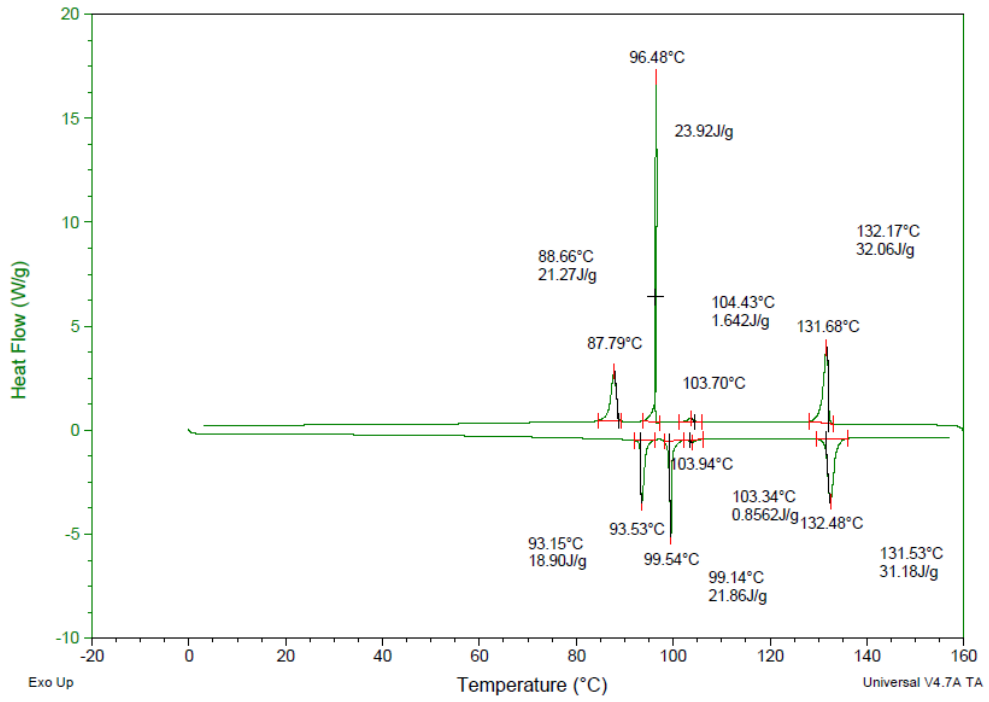

179

180 **Figure S18.** DSC thermogram of **Th-Thd-Th(12)**.

181 **5. Thermogravimetric Analysis (TGA)**

182 Thermogravimetric analysis was carried out on a Shimadzu TGA-50 with a heating rate of 2 °C
183 per minute.

184 TGA of Th-Oxd-Th(10):

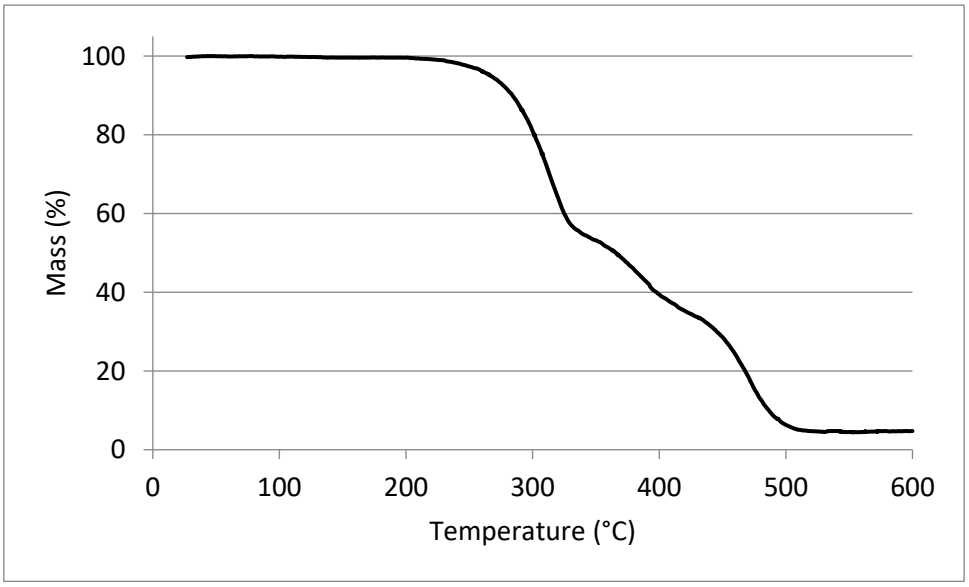

185

186 TGA of Th-Thd-Th(4):

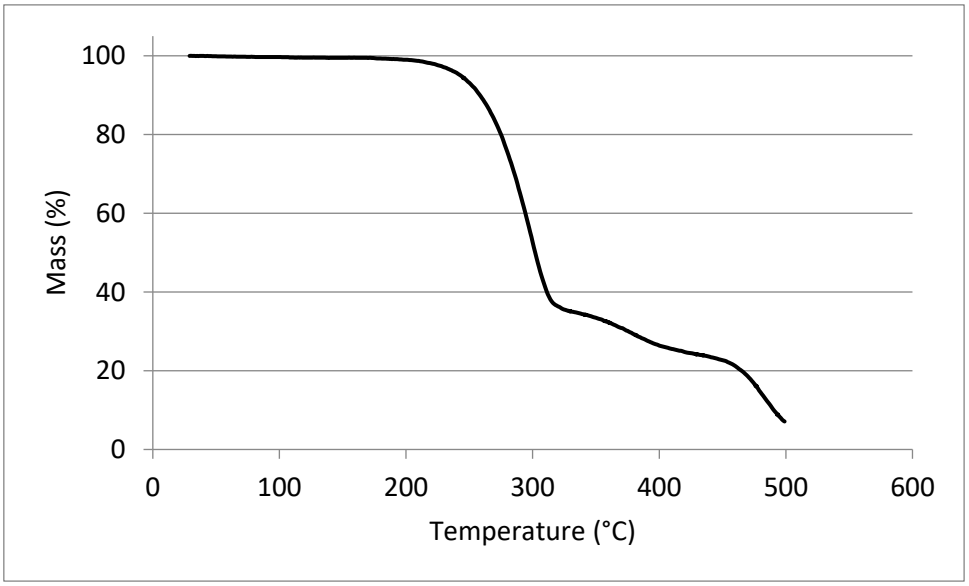

187

188 TGA of Th-Thd-Th(6):

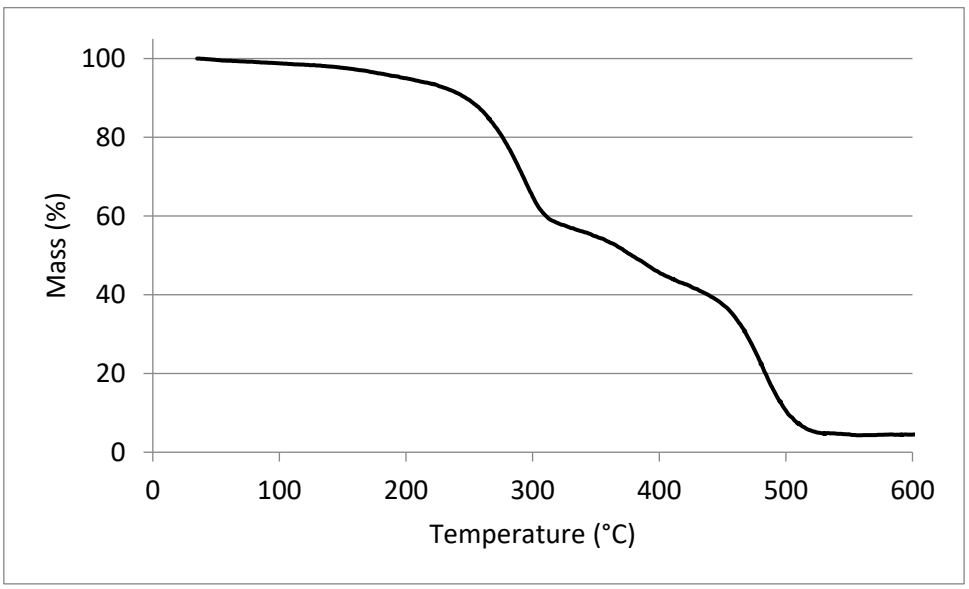

189

190 TGA of Th-Thd-Th(8):

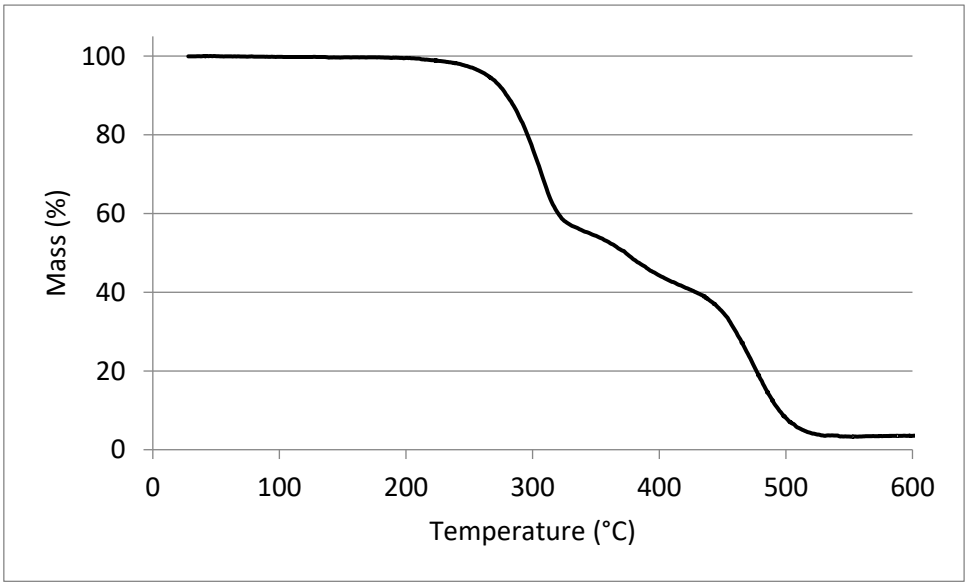

191

192 TGA of Th-Thd-Th(10):

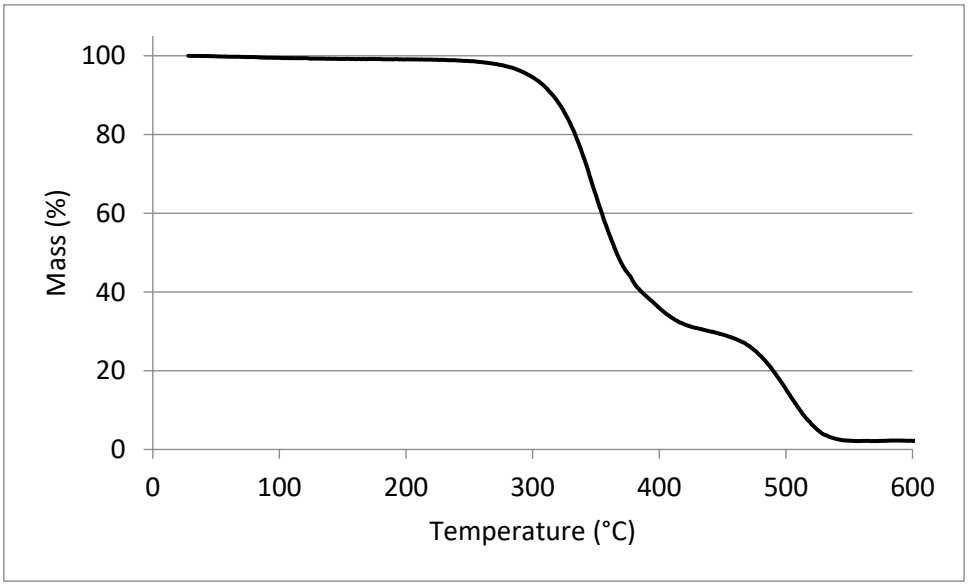

193

194 TGA of Th-Thd-Th(12):

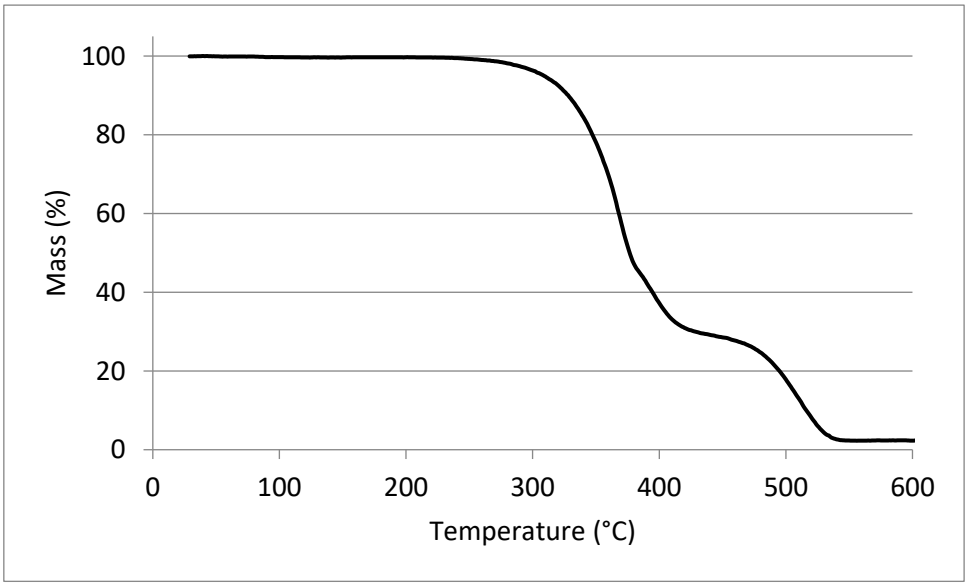

195

196 **6. Single Crystal X-ray Diffraction**

197 Suitable crystals (**Th-Thd-Th**, **Th-Thd-Th(4)** and **Th-Thd-Th(10)**) were coated in paratone oil,
198 mounted on a MiTeGen Micro Mount, and transferred to the the X-ray diffractometer. Data was
199 collected on a Bruker Smart instrument equipped with an APEX II CCD area detector fixed at a
200 distance of 5.0 cm (**Th-Thd-Th**, **Th-Thd-Th(4)**) or 4.0 cm (**Th-Thd-Th(10)**), from the crystal and a Cu
201 Kα fine focus sealed tube (λ = 1.54178 Å) operated at 1.5 kW (45 kV, 0.65 mA), filtered with a graphite
202 monochromator. Data was collected at 150K (**Th-Thd-Th(4)**, **Th-Thd-Th(10)**) or 296K (**Th-Thd-Th**);
203 the temperature was regulated using an Oxford Cryosystems Cryostream. Additional
204 crystallographic information can be found in Table S4. All diffraction data were processed using the
205 Bruker SAINT software package and were corrected for absorption effects using the multi-scan
206 technique (SADABS [3] or TWINABS [4]). The structures were solved with direct methods (SIR92)
207 and subsequent refinements were performed using SHELXL [5] and ShelXle. [6] Hydrogen atoms on
208 carbon atoms were included at geometrically idealized positions (C–H bond distance 0.95Å) and
209 were not refined. The isotropic thermal parameters of the hydrogen atoms were fixed at 1.2 times
210 that of the preceding carbon atom. Diagrams were prepared using ORTEP-3 [7] and POV-RAY. [8]
211 Thermal ellipsoids are shown at the 50% probability level.

212 **Table S4.** Crystallographic information table for **Th-Thd-Th**, **Th-Thd-Th(4)**, and **Th-Thd-Th(10)**.

Compound	**Th-Thd-Th**	**Th-Thd-Th(4)**	**Th-Thd-Th(10)**
Chemical Formula	$C_{10}H_6N_2S_3$	$C_{18}H_{22}N_2S_3$	$C_{30}H_{46}N_2S_3$
Formula Mass	250.35	362.55	530.87
a/Å	6.34810(10)	7.3146(4)	7.5511(11)
b/Å	9.63630(10)	7.6299(3)	9.6532(16)
c/Å	17.8284(2)	18.0456(9)	23.523(4)
α/°	90	85.306(4)	91.278(8)
β/°	94.9750(10)	84.800(4)	94.604(7)
γ/°	90	67.452(4)	100.468(9)
Unit cell volume/Å^3	1086.49(2)	925.09(8)	1679.5(5)
Temperature/K	159(2)	150(2)	150(2)
Space group	P21/c	P-1	P-1

Number of formula unit per cell/Z	4	2	2
Radiation type	Cu Kα	Cu Kα	Cu Kα
Absorption coefficient, μ/mm^{-1}	5.949	3.651	2.142
No. of reflections collected	5857	9288	17667
No. unique reflections	1922	3161	5526
R_{int}	0.0288	0.0693	0.0630
Final R_1 values (I>2σ(I))	0.0449	0.0867	0.2077
Final wR(F^2) values (I>2σ(I))	0.1299	0.2800	0.5868
Final R_1 values (all data)	0.0475	0.1088	0.2178
Final wR(F^2) (all data)	0.1331	0.2965	0.6060
Goodness of fit	1.080	1.161	3.232

All crystal structure figures below follow the legend: sulphur in yellow, nitrogen in light blue, carbon in grey, hydrogen in white.

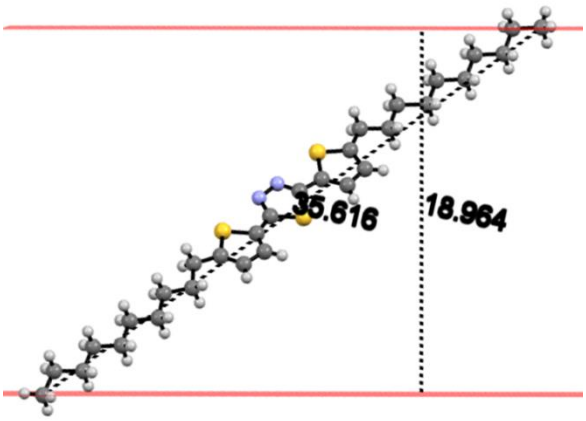

Figure S19. Estimation of the tilt angle in the room temperature smectic phase of **Th-Thd-Th(10)** based on the single crystal structure.

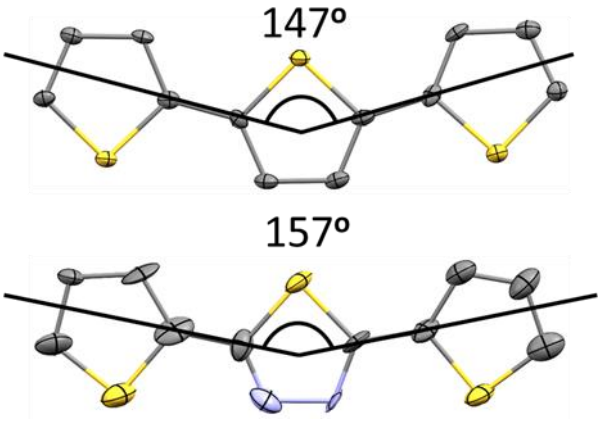

Figure S20. Bond angles at the 2 and 5 positions of the central heterocycle for **Th$_3$(8)**[9] and **Th-Thd-Th(10)**. Alkyl chains and hydrogens omitted for clarity.

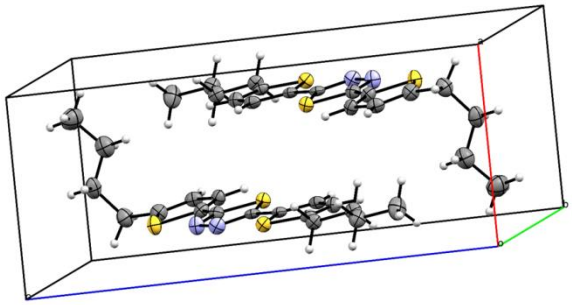

(a)

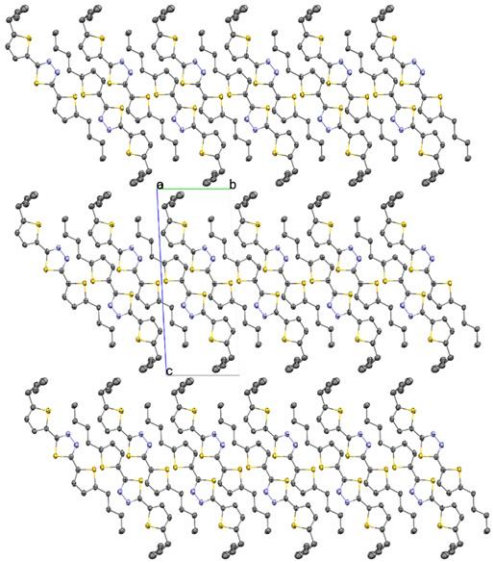

(b)

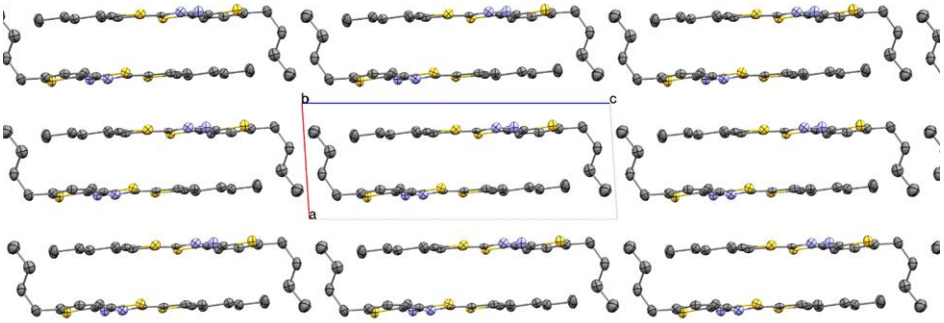

(c)

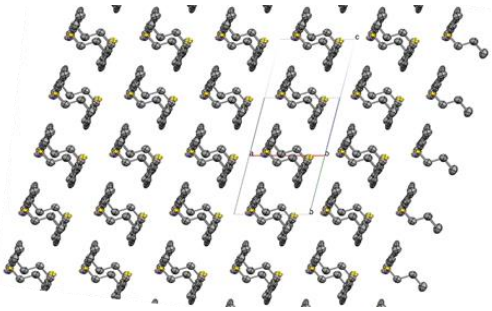

(d)

Figure S21. Single crystal structure of **Th-Thd-Th(4)** showing the unit cell (a), lamellar order looking down the a- or b- axis (b and c respectively), and intra-layer packing looking down the c-axis (d).

a)

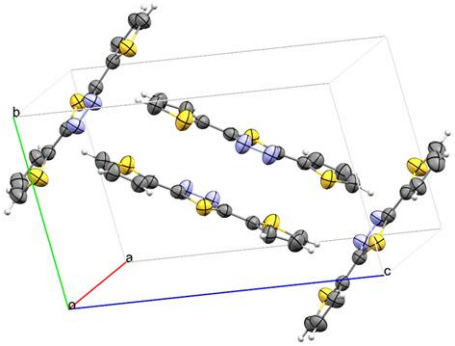

b)

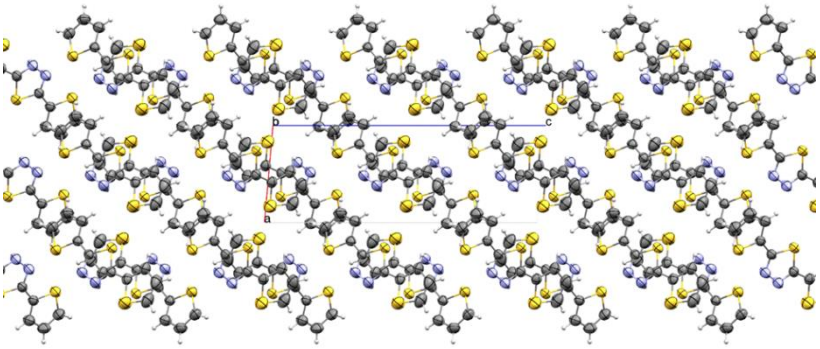

c)

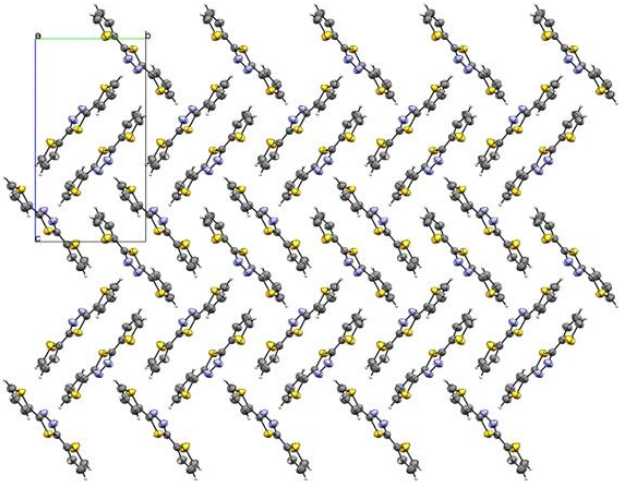

Figure S22. Single crystal structures of **Th-Thd-Th** showing the unit cell (a), order looking down the b-axis (b), and herringbone packing looking down the a-axis (c).

a)

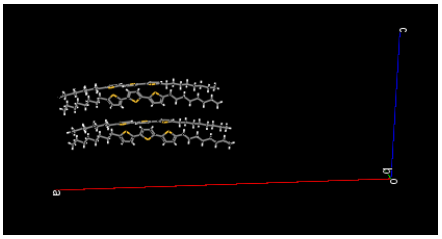

b)

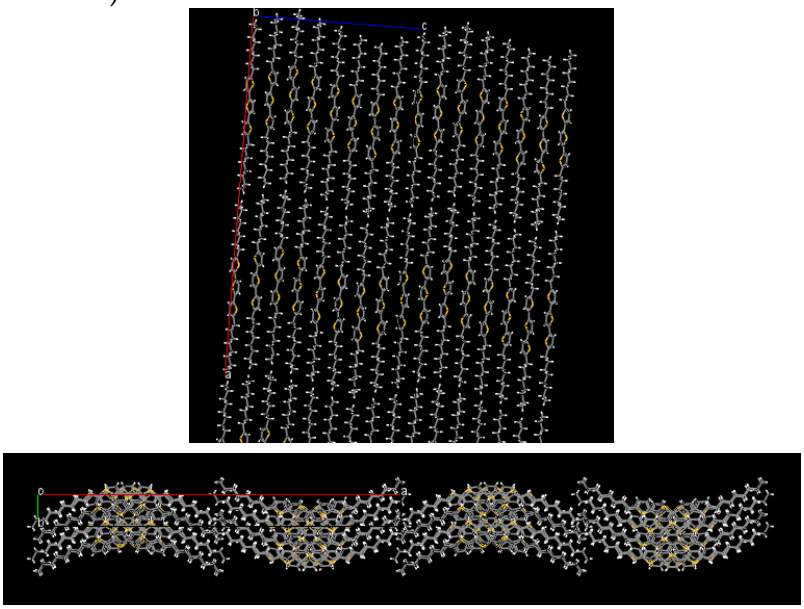

c)

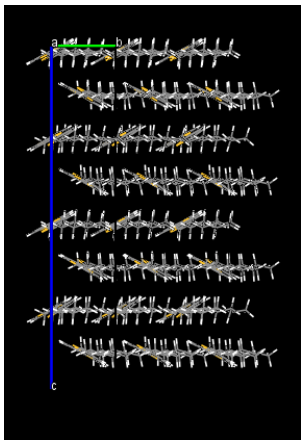

225 **Figure S23.** Literature single crystal structures of **Th$_3$(8)**[9] showing the unit cell (a), lamellar order
226 (b), and intra-layer packing (c).

a)

b)

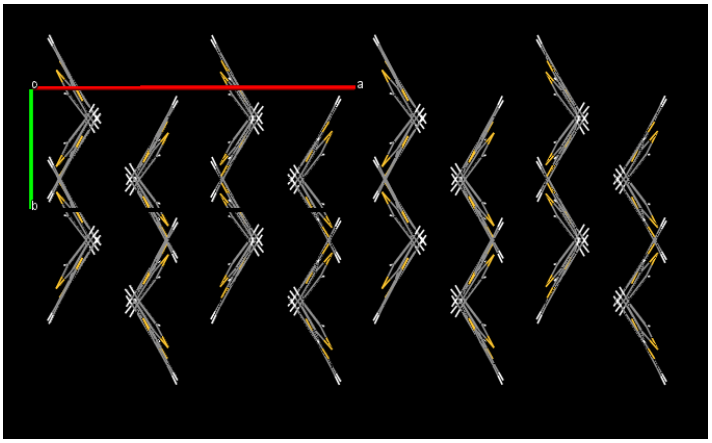

Figure S24. Literature single crystal structures of **Th3**[10] showing the unit cell (a) and herringbone packing (b).

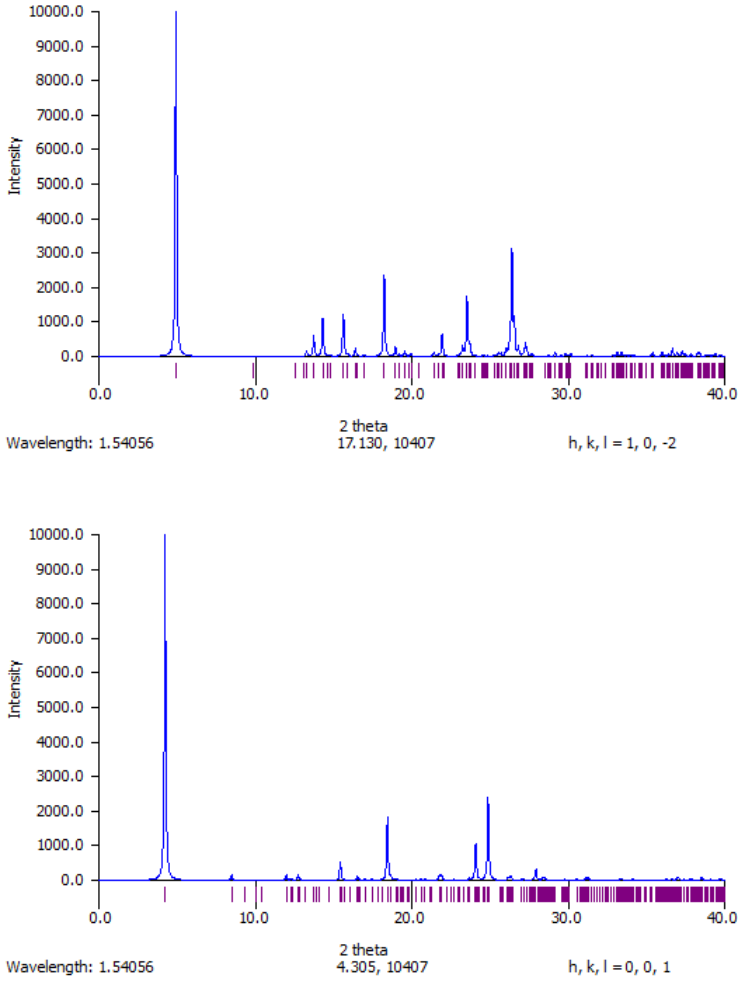

Figure S25. Simulated powder XRD patterns of **Th-Thd-Th(4)** (a) and **Th-Thd-Th(10)** (b) as determined based on the single crystal structure.

7. UV/vis Absorption Spectroscopy

Table S5. Summary of UV-Vis spectral properties.

Compound	λ_{abs}^{max} (nm)	ε ($M^{-1}cm^{-1}$)	λ_{abs}^{onset} (nm)	E_g^{opt} (eV)[a]

Th-Oxd-Th(10)	328	28200	371	3.35
Th-Thd-Th(10)	359	26800	409	3.04
Th$_3$(10)	367	25900	423	2.93

[a]Optical bandgap, estimated by $E_g = hc/\lambda_{abs}^{onset}$

a)

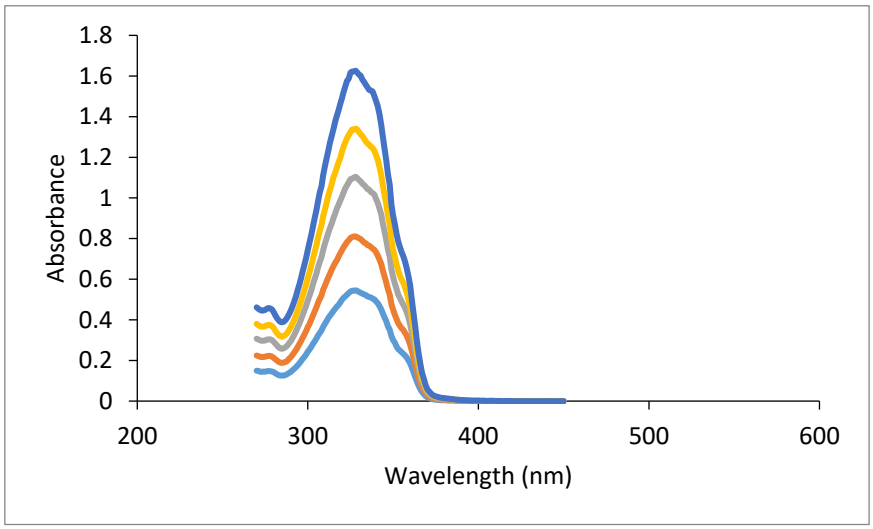

b)

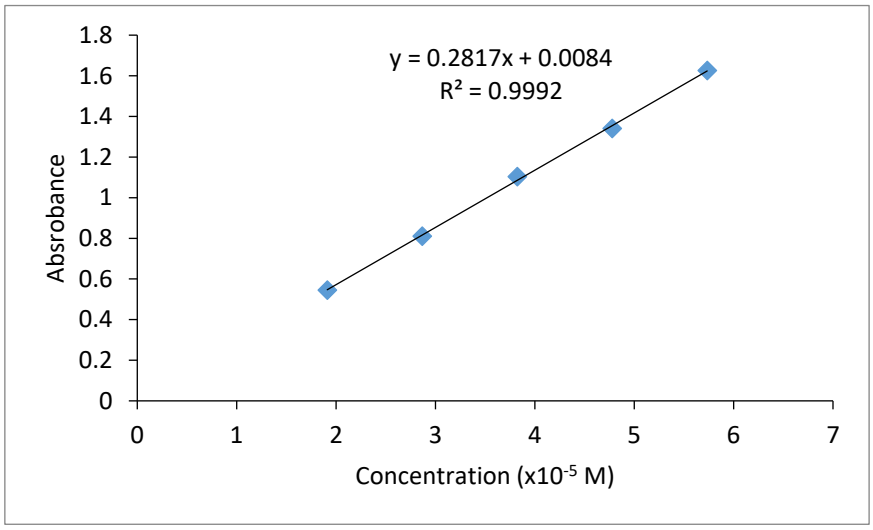

Figure S26. Absorption spectra of **Th-Oxd-Th(10)** in chloroform at various concentrations ranging from around 6x10^{-5} to 2x10^{-5} M (top to bottom) (a) and the resulting Beer-Lambert plot (b).

a)

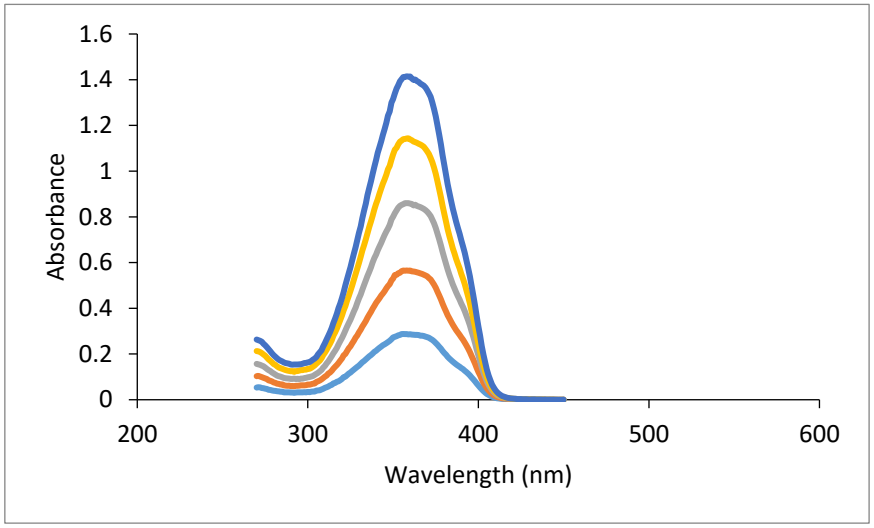

b)

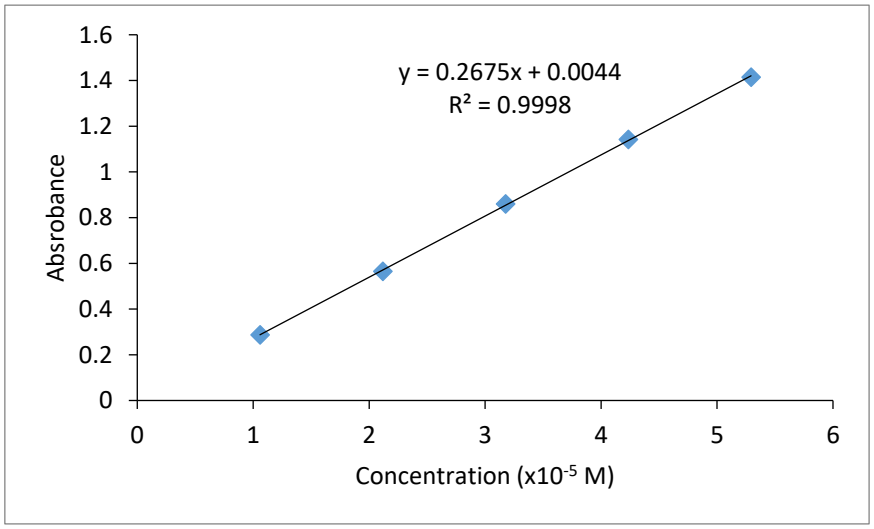

236 **Figure S27.** Absorption spectra of **Th-Thd-Th(10)** in chloroform at various concentrations ranging
237 from around 5×10^{-5} to 1×10^{-5} M (top to bottom) (a) and the resulting Beer-Lambert plot (b).

a)

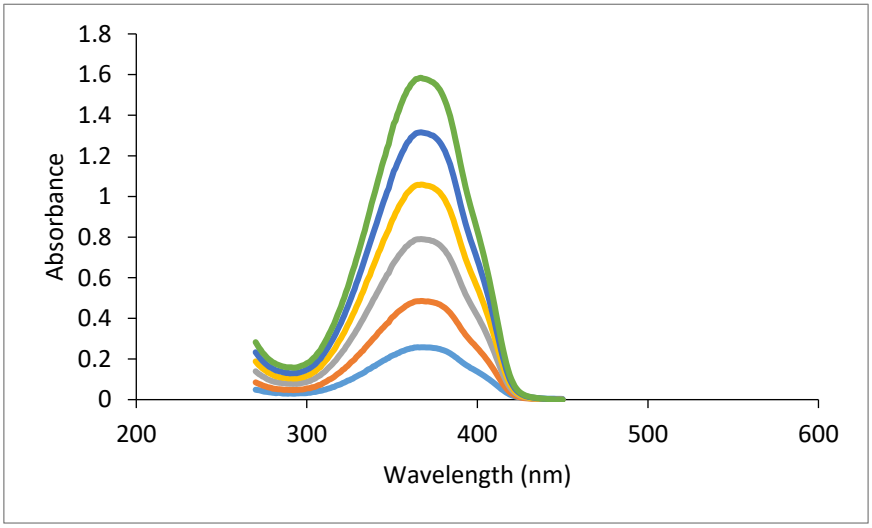

b)

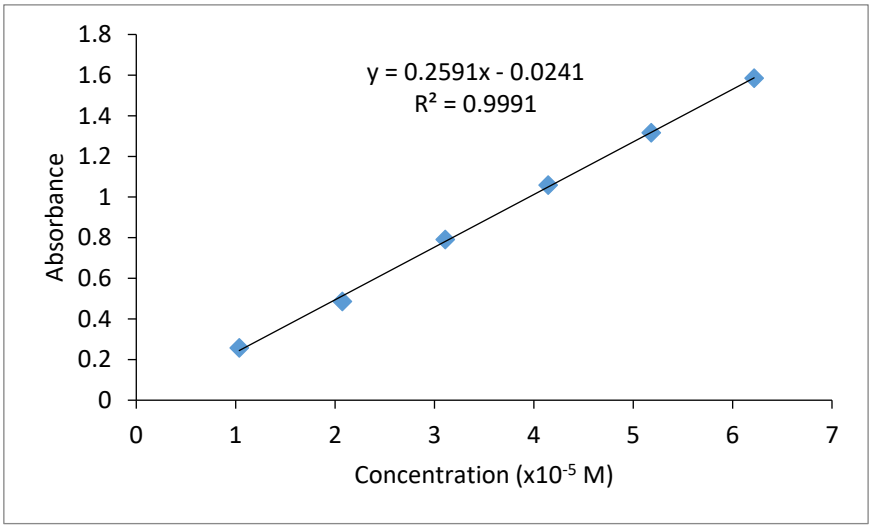

Figure S28. Absorption spectra of **Th₃(10)** in chloroform at various concentrations ranging from around 6 × 10^{-5} to 1 × 10^{-5} M (top to bottom) (a) and the resulting Beer-Lambert plot (b).

8. Fluorescence Excitation/Emission Spectroscopy

Table S6. Summary of fluorescence spectral properties.

Compound	λ_{ex}^{max} (nm)[a]	λ_{em}^{max} (nm)[b]	Stokes shift (nm)	Φ_f[c]
Th-Oxd-Th(10)	340	387	47	0.48
Th-Thd-Th(10)	369	430	61	0.49
Th₃(10)	380	443	63	0.56

[a] Observed at the corresponding λ_{em}^{max} ; [b] Measured at the respective λ_{ex}^{max} ; [c] Relative to quinine sulfate standard (Φ_f = 0.54) in 0.1 M H_2SO_4

Table S7. Detailed fluorescence data used for quantum yield determination.

Compound	Concentration (x10^{-6} M)	Maximum absorbance, A_{max}	Integrated emission intensity, I_{em}	I_{em}/A_{max} gradient[a]	Φ_f[b]
Th-Oxd-Th(10)	0.96	552038	43751369	74.9	0.48
	1.91	898329	69736325		
	2.87	1235771	94299072		
	3.82	1567427	119646050		
	4.78	1915589	145914659		
Th-Thd-Th(10)	2.12	275332	21930717	76.4	0.49
	6.35	559616	43049313		

	8.47	696109	53070730		
	10.59	828772	63336304		
	12.70	983655	75462409		
	16.94	1258332	97024851		
Th_3(10)	0.52	376360	38399486	87.1	0.56
	0.62	423623	42422719		
	0.73	526075	51875681		
	0.83	599034	58557104		
	0.93	685502	64905104		
Quinine sulfate	6.65	622805	59563561	98.2	0.54
	8.87	792582	76626907		
	11.09	985531	93600171		
	13.30	1151426	110217780		
	15.52	1305979	126343550		
	17.74	1459479	142261748		

[a] Determined from slope of I_{em} vs. A_{max} at various concentrations, see plots below; [b] Calculated according to: $\Phi_{f,x} = \Phi_{f,ref} (I_{em,x}/A_{max,x}) (A_{max,ref} /I_{em,ref}) (\eta_x /\eta_{ref})^2$,[11] using the quinine sulfate standard ($\Phi_f = 0.54$)[12] in 0.1 M H_2SO_4, the gradients above determined from experiment, and $\eta_{chloroform} = 1.444$ and $\eta_{water} = 1.333$.

a)

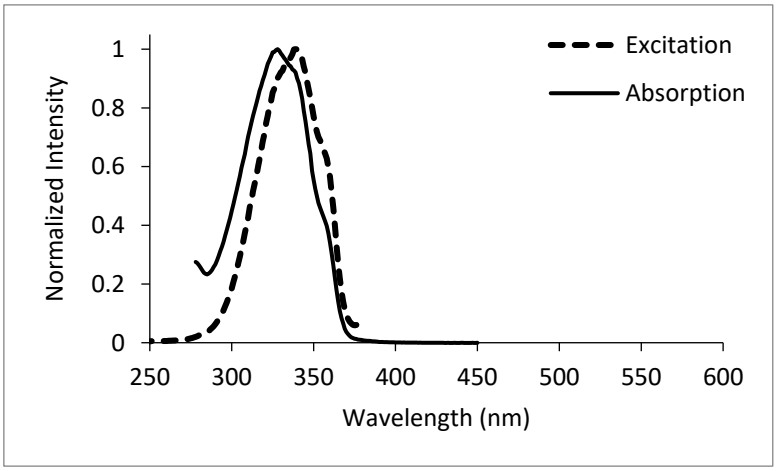

b)

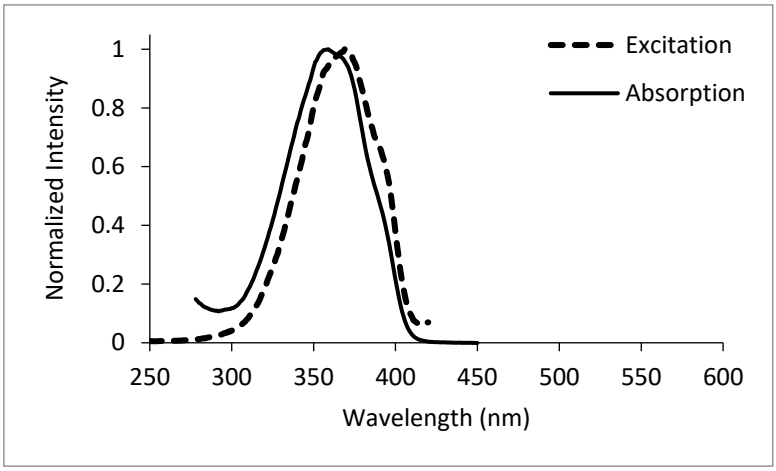

c)

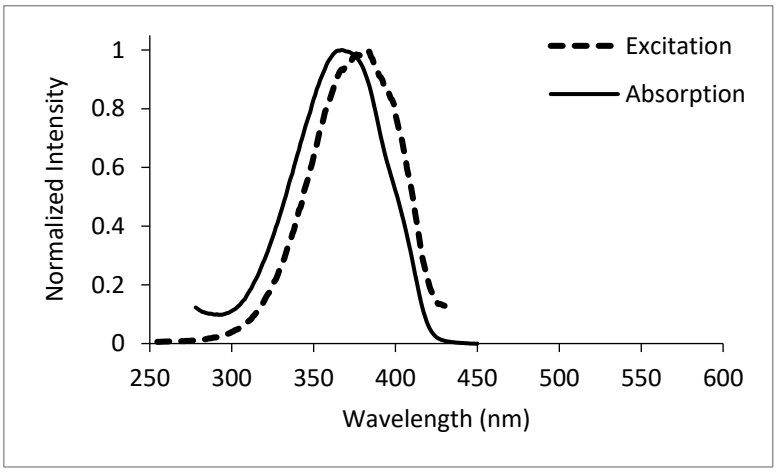

Figure S29. Overlay of UV/vis absorption (solid line) and fluorescence excitation (dashed line) spectra of **Th-Oxd-Th(10)** (a), **Th-Thd-Th(10)** (b), and **Th$_3$(10)** (c) in $CHCl_3$.

a)

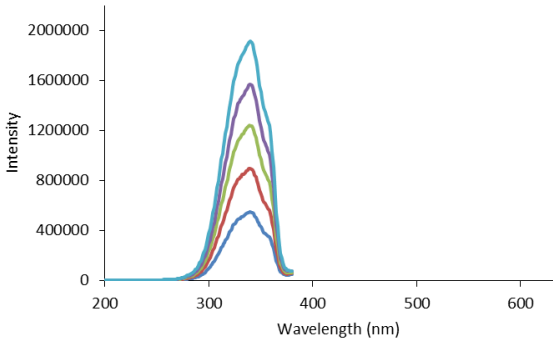

b)

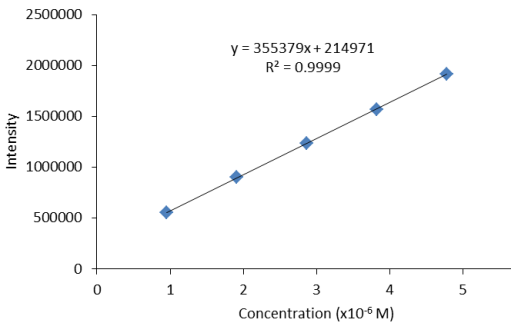

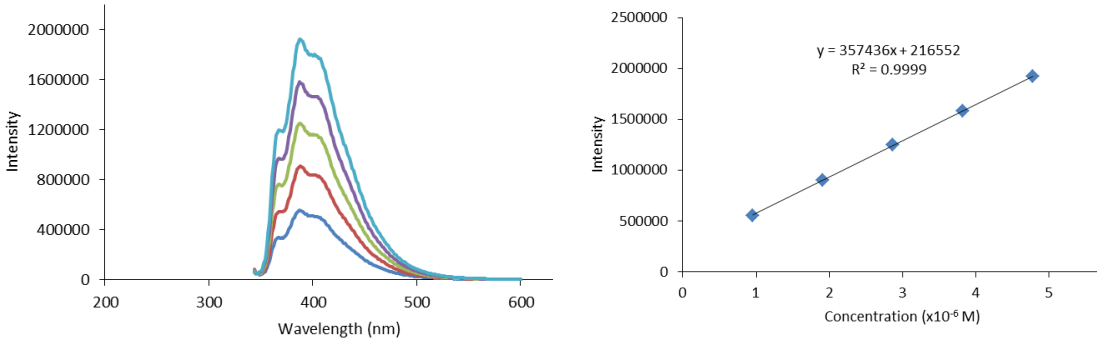

Figure S30. Fluorescence excitation (top) and emission (bottom) spectra of **Th-Oxd-Th(10)** in chloroform at various concentrations ranging from around 5 x 10^{-6} to 1x10^{-6} M (shown in descending order) (a) and the respective Beer-Lambert plots demonstrating the linear range (b).

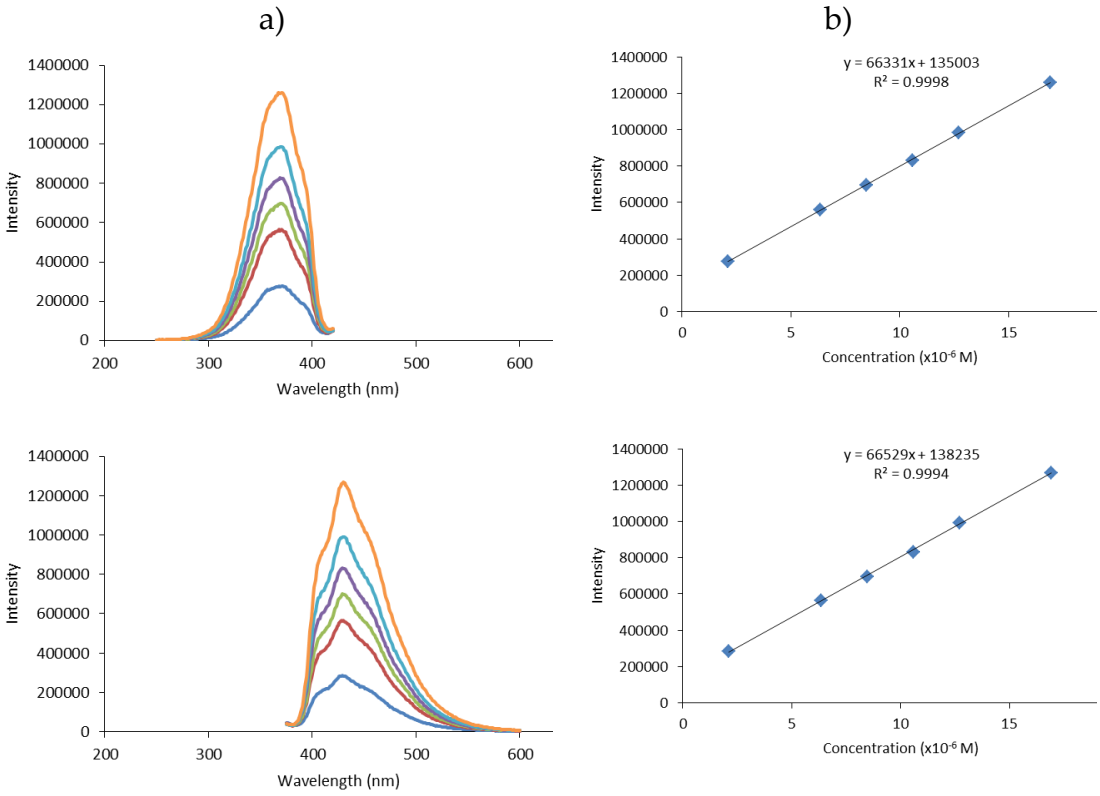

Figure S31. Fluorescence excitation (top) and emission (bottom) spectra of **Th-Thd-Th(10)** in chloroform at various concentrations ranging from around 16 × 10^{-6} to 2 × 10^{-6} M (shown in descending order) (a) and the respective Beer-Lambert plots demonstrating the linear range (b).

a) b)

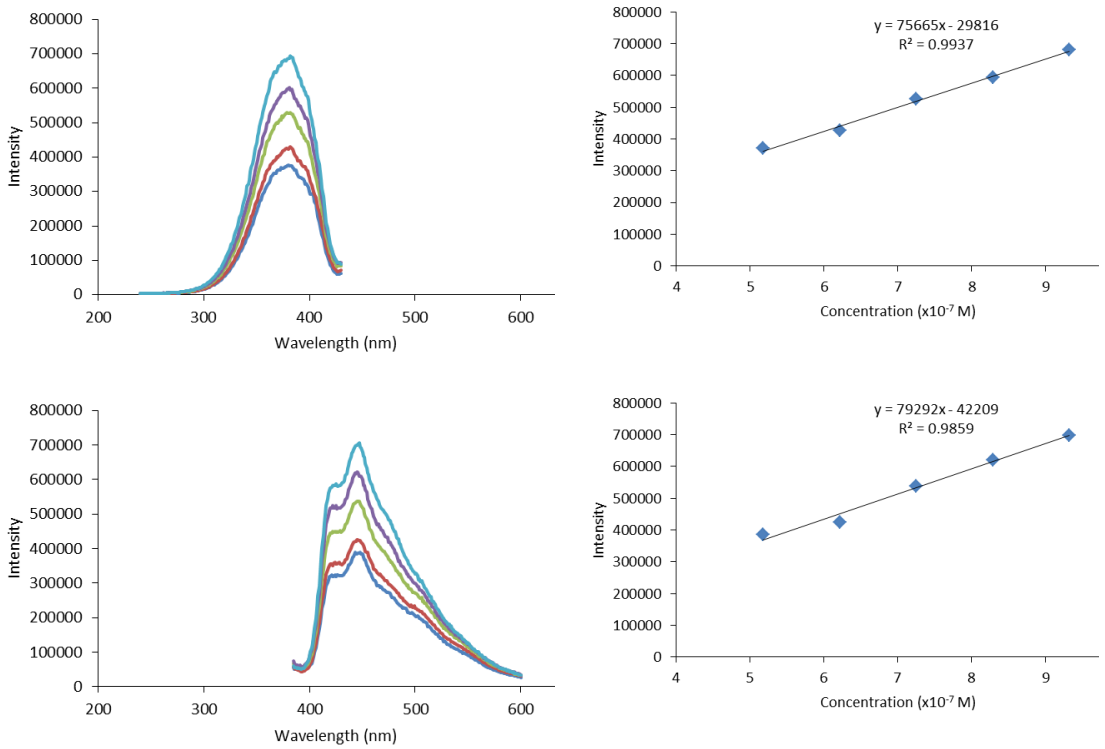

Figure S32. Fluorescence excitation (top) and emission (bottom) spectra of **Th_3(10)** in chloroform at various concentrations ranging from around 9×10^{-7} to 5×10^{-7} M (shown in descending order) (a) and the respective Beer-Lambert plots demonstrating the linear range (b).

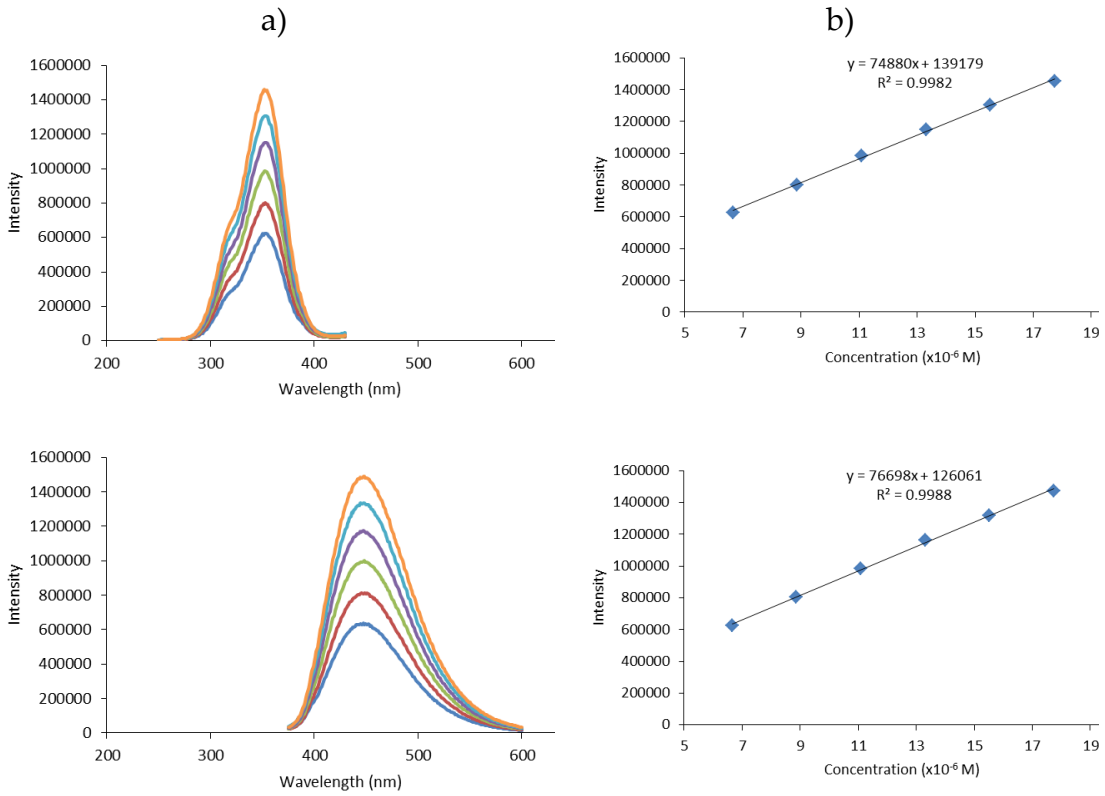

Figure S33. Fluorescence excitation (top) and emission (bottom) spectra of quinine sulfate in 0.1 M sulfuric acid at various concentrations ranging from around 17×10^{-6} to 6×10^{-6} M (shown in descending order) (a) and the respective Beer-Lambert plots demonstrating the linear range (b).

a)

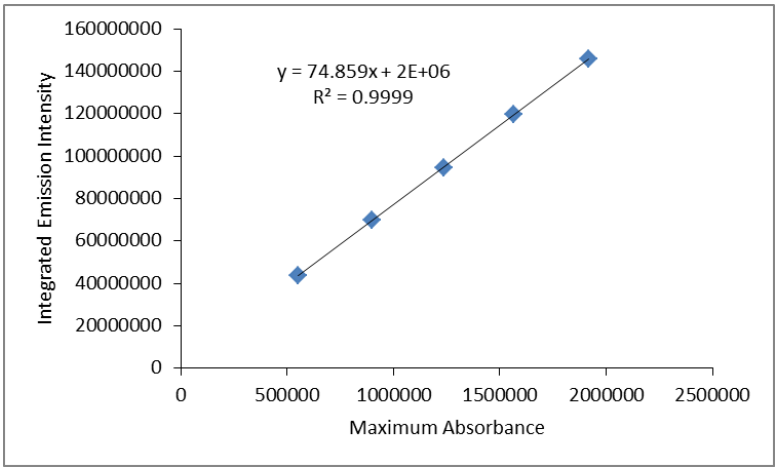
y = 74.859x + 2E+06
R² = 0.9999
Integrated Emission Intensity
Maximum Absorbance
160000000
140000000
120000000
100000000
80000000
60000000
40000000
20000000
0
0
500000
1000000
1500000
2000000
2500000

b)

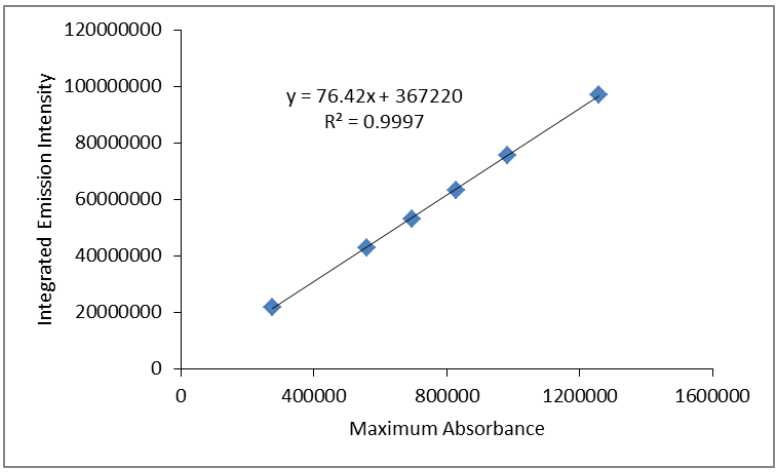
y = 76.42x + 367220
R² = 0.9997
Integrated Emission Intensity
Maximum Absorbance
120000000
100000000
80000000
60000000
40000000
20000000
0
0
400000
800000
1200000
1600000

c)

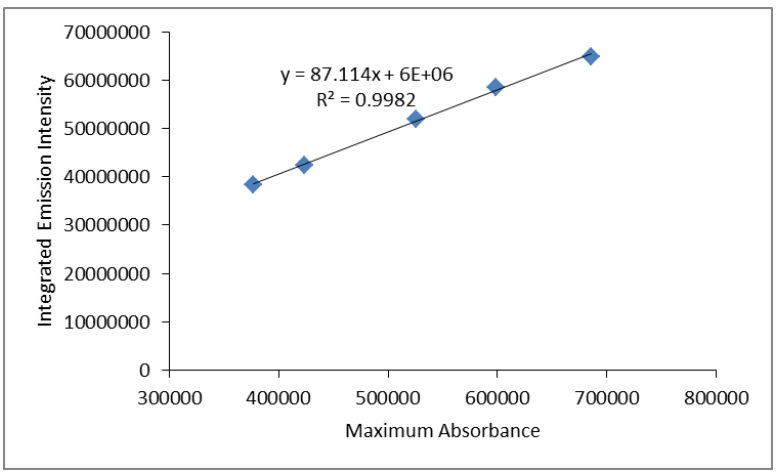
y = 87.114x + 6E+06
R² = 0.9982
Integrated Emission Intensity
Maximum Absorbance
70000000
60000000
50000000
40000000
30000000
20000000
10000000
0
300000
400000
500000
600000
700000
800000

d)

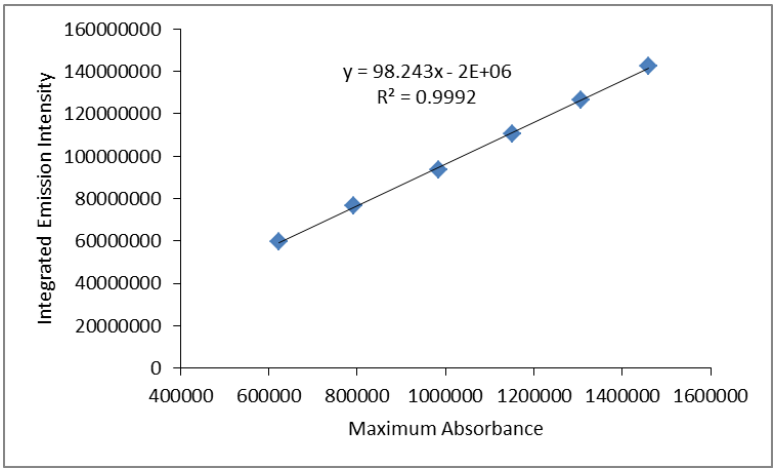

Figure S34. Integrated emission intensity vs. maximum absorbance plots created based on the fluorescence spectra at various concentrations shown above for **Th-Oxd-Th(10)** (a), **Th-Thd-Th(10)** (b), **Th$_3$(10)** (c), and quinine sulfate (d).

9. Cyclic Voltammetry (CV)

Cyclic voltammetry scans were performed on a PAR-263A potentiometer. All analytes were scanned as 1.0 mM solutions in THF (**Th-Ox-Th(10)** and **Th-Thd-Th(6)** reduction) or MeCN (**Th-Thd-Th(6)** oxidation) with a 0.1 M tetrabutylammonium perchlorate supporting electrolyte. The apparatus was a 20 ml glass cell equipped with a glassy carbon working electrode, platinum counter electrode and silver wire reference electrode. All scans were reference internally to a Fc/Fc^+ reversible redox couple.

Table S8. Summary of the raw CV data for select compounds.

Compound	Process/ solvent	Analyte (compound)			Ferrocene reference		
		E_a (V)	E_c (V)	$E^{1/2}$ (V)[a]	E_a (V)	E_c (V)	$E^{1/2}$ (V)
Th-Oxd-Th(10)	Reduction/ THF	n/a, irreversible		-2.20	1.29	0.53	0.91
Th-Thd-Th(6)	Reduction/ THF	-1.32	-1.64	-1.48	1.35	0.50	0.93
	Oxidation/ MeCN	n/a, irreversible		1.92	0.92	0.56	0.74

[a] Irreversible processes estimated based on middle of onset slope

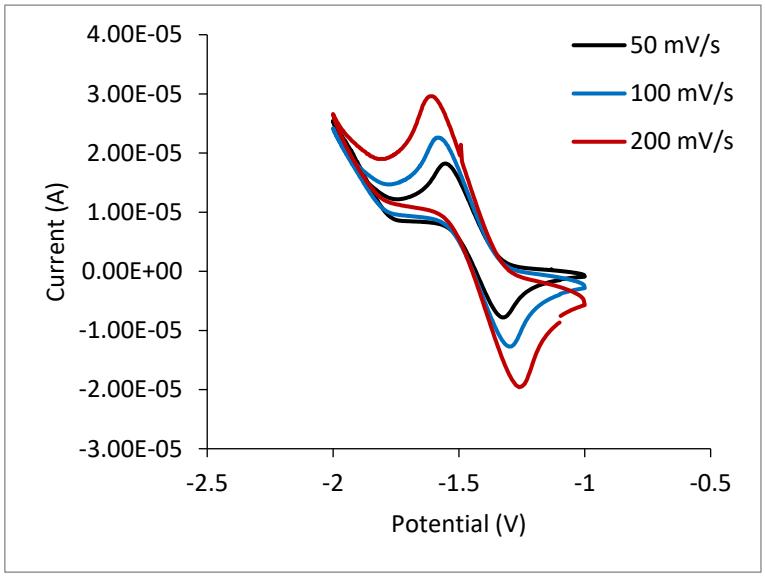

276

277 **Figure S35.** Unprocessed cyclic voltammograms showing the reversible reduction of **Th-Thd-Th(6)**
278 at different scan rates.

a)

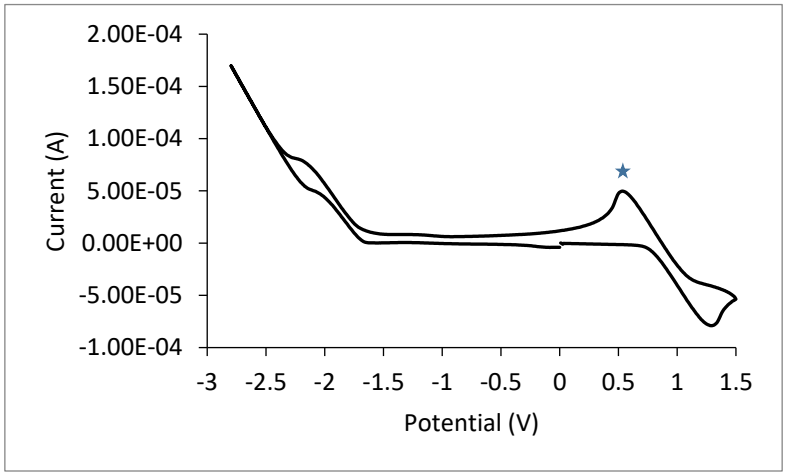

b)

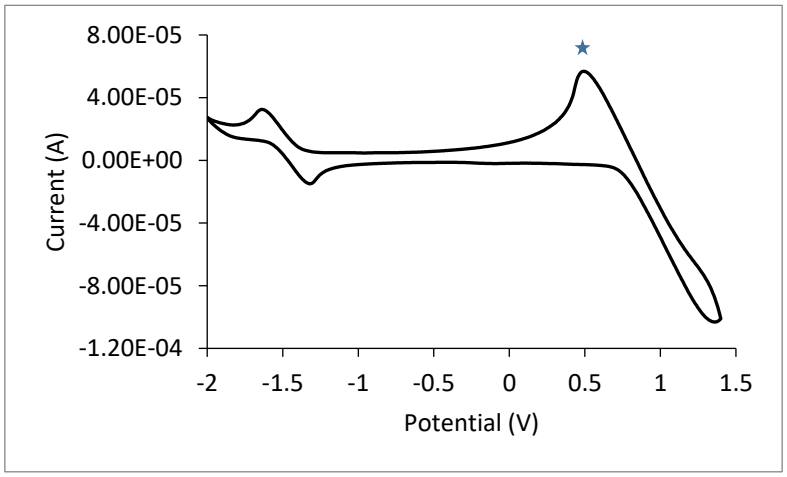

c)

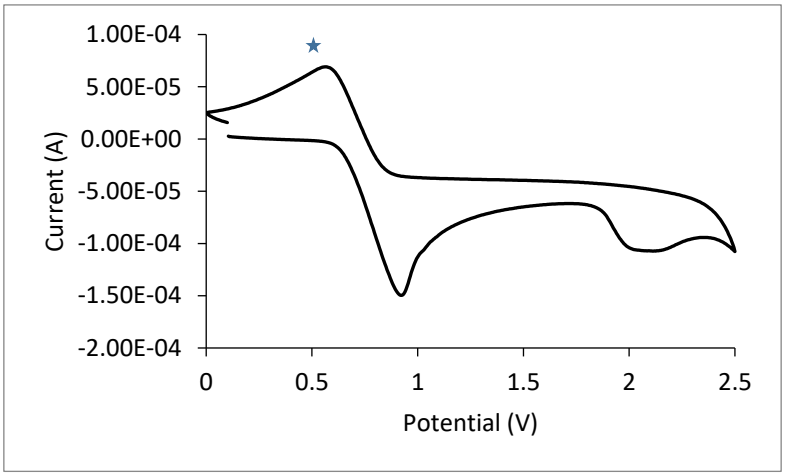

Figure S36. Unprocessed cyclic voltammograms showing the ferrocene internal standard signal (blue star) used for reference for **Th-Oxd-Th(10)** reduction in THF (a), **Th-Thd-Th(6)** reduction in THF (b), and **Th-Thd-Th(6)** oxidation in MeCN (c).

10. DFT and TD-DFT Calculations

Density functional theory (DFT) – DFT calculations were carried out using B3LYP functional[13,14] and 6-31G* basis set (C, H, N, O, S)[15–18] in Gaussian 16[19] to determine the optimized molecular structures (Figure 6) as well as the frontier molecular orbitals and respective HOMO/LUMO energy levels (Figure S36). All of these results were consistent with those obtained by different basis sets used during TD-DFT calculations (see following).

Time-dependent density functional theory (TD-DFT) – Geometry optimization calculations were completed using the Gaussian 16 program (Revision B.01)[19], the restricted B3LYP functional[13,14], the 6-31G* basis set (C, H, N, O, S), with a polarized continuum model (PCM) for $CHCl_3$ (dielectric ε = 4.9).[15–18] Frequency calculations at the same level of theory confirmed that the optimized structures were located at a minimum on the potential energy surface. Single-point calculations were done using restricted B3LYP functional, the TZVP basis set (C, H, N, O, S)[20,21], with a PCM for $CHCl_3$. The intensities of 30 lowest energy transitions using TD-DFT[22,23] calculations were performed using the CAM-B3LYP functional[24–26], the TZVP basis set (C, H, N, O, S), with a PCM for $CHCl_3$.

Table S9. Summary of predicted properties determined by DFT (B3LYP/6-31G*).

Compound	Gas phase			Solvated in THF		
	HOMO (eV)	LUMO (eV)	E_g^{calc} (eV)	HOMO (eV)	LUMO (eV)	E_g^{calc} (eV)
Th_3(10)	-4.88	-1.51	3.37	-5.05	-1.69	3.36
Th-Oxd-Th(10)	-5.59	-1.62	3.97	-5.77	-1.80	3.97
Th-Thd-Th(10)	-5.54	-1.90	3.64	-5.71	-2.08	3.62
Th-Thd-Th(6)	-5.54	-1.90	3.64	-5.71	-2.09	3.62

Table S10. Summary of predicted properties determined by TD-DFT (CAM-B3LYP/TZVP).

Compound	TD-DFT

	λ_{abs}^{max} (nm)	f[a]	E_g^{opt} (eV)[b]
Th_3(10)	383	1.15	2.67
Th-Oxd-Th(10)	323	1.16	3.26
Th-Thd-Th(10)	354	1.18	2.94

[a] Oscillator strength

[b] Optical bandgap, estimated by $E_g = hc/\lambda_{abs}^{onset}$

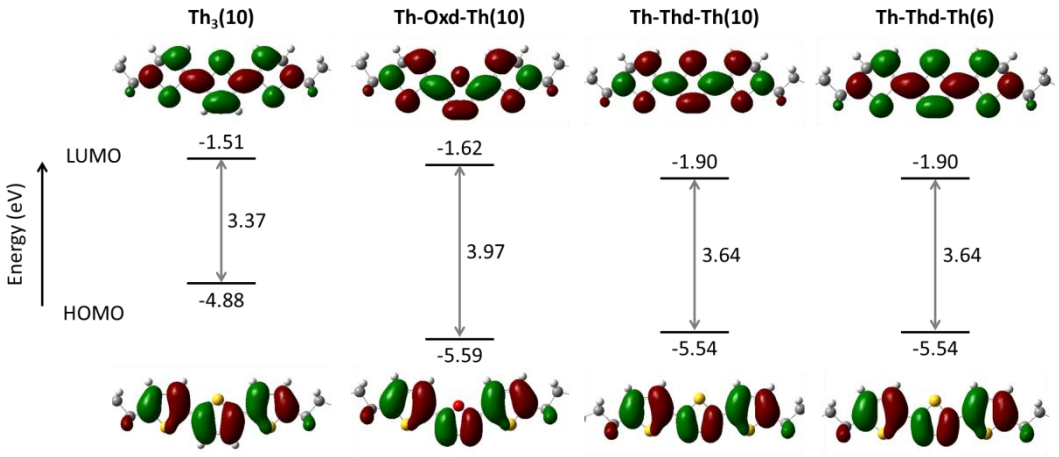

Figure S37. Frontier molecular orbitals of select compounds calculated by DFT at B3LYP/6-31G* level.

a)

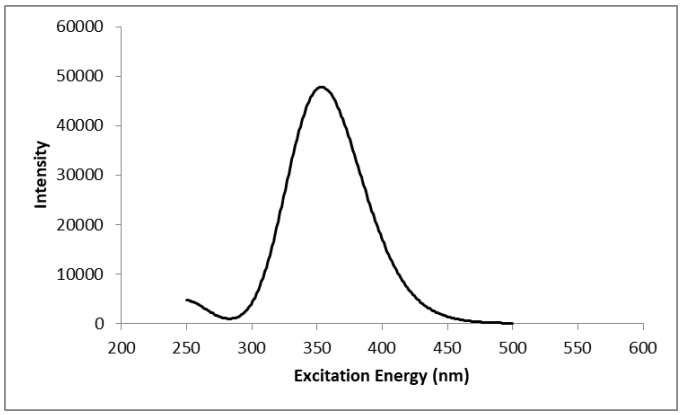

b)

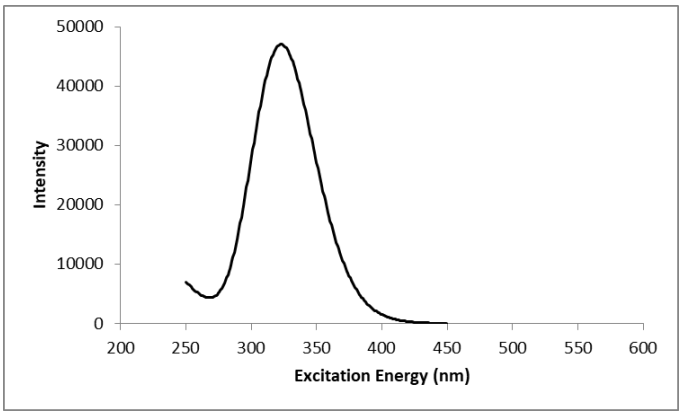

c)

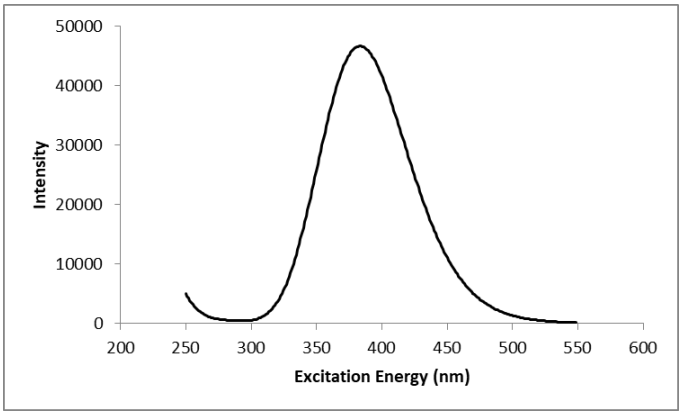

Figure S38. TD-DFT predicted UV/vis spectra in chloroform of **Th_3(10)** (a), **Th-Oxd-Th(10)** (b), and **Th-Thd-Th(10)** (c).

11. Complete List of Computational Data

Optimized coordinates (Å) for Th-Oxd-Th(10):

C	1.06861315	-2.08694106	0.00077733
C	-1.06861352	-2.08694115	0.00071126
C	2.39766853	-1.54132287	-0.00139990
C	2.77436144	-0.21785222	-0.00711548
S	3.79545595	-2.59381429	0.00380009
C	4.18572883	-0.04510711	-0.00774990
H	2.06185720	0.59918123	-0.01079215
C	4.88823187	-1.22612957	-0.00253064
H	4.66347744	0.92751470	-0.01198087
C	-2.39766880	-1.54132337	-0.00161983
C	-2.77436145	-0.21785256	-0.00731636
S	-3.79545651	-2.59381625	0.00318546
C	-4.18572881	-0.04510757	-0.00804950
H	-2.06185703	0.59918136	-0.01084878
C	-4.88823212	-1.22613025	-0.00291490
H	-4.66347720	0.92751460	-0.01222002
N	0.69495173	-3.33705542	0.00614971
N	-0.69495230	-3.33705639	0.00589109
C	6.37730125	-1.45485264	-0.00210701
H	6.64913616	-2.06181825	0.87321688

331	H	6.64960845	-2.06146371	-0.87757292
332	C	7.21222653	-0.16644298	-0.00169072
333	H	6.95424034	0.43684545	-0.88254785
334	H	6.95256581	0.43731071	0.87835320
335	C	8.72046191	-0.44679165	-0.00034091
336	H	8.97778842	-1.05622778	-0.87899553
337	H	8.97639213	-1.05525476	0.87939382
338	C	9.57263471	0.82886404	-0.00039303
339	H	9.31489655	1.43723484	-0.87997259
340	H	9.31352133	1.43825006	0.87807735
341	C	11.08204180	0.55434118	0.00093129
342	H	11.34045757	-0.05583227	-0.87730798
343	H	11.33914876	-0.05461481	0.88039787
344	C	11.93592221	1.82897310	0.00067000
345	H	11.67705214	2.43912377	0.87889034
346	H	11.67831709	2.43789854	-0.87877272
347	C	13.44553753	1.55547064	0.00193890
348	H	13.70423043	0.94509834	-0.87622063
349	H	13.70300327	0.94644163	0.88139028
350	C	14.30000861	2.82952366	0.00155407
351	H	14.04226918	3.44048647	0.87974964
352	H	14.04348258	3.43913280	-0.87793698
353	C	15.80965123	2.55653223	0.00280353
354	H	16.06751629	1.94662021	-0.87482891
355	H	16.06631717	1.94801871	0.88175698
356	C	-6.37730151	-1.45485311	-0.00253797
357	H	-6.64960136	-2.06129019	-0.87812652
358	H	-6.64914399	-2.06199258	0.87266316
359	C	-7.21222663	-0.16644339	-0.00187290
360	H	-6.95422436	0.43702490	-0.88260214
361	H	-6.95258163	0.43713048	0.87829899
362	C	-8.72046207	-0.44679200	-0.00060999
363	H	-8.97641050	-1.05543125	0.87899758
364	H	-8.97777064	-1.05605206	-0.87939196
365	C	-9.57263461	0.82886387	-0.00042410
366	H	-9.31487576	1.43741292	-0.87987429
367	H	-9.31354154	1.43807172	0.87817585
368	C	-11.08204175	0.55434112	0.00080914
369	H	-11.33916919	-0.05479501	0.88014500
370	H	-11.34043741	-0.05565229	-0.87756110
371	C	-11.93592184	1.82897329	0.00078963
372	H	-11.67829497	2.43808021	-0.87852102
373	H	-11.67707320	2.43894256	0.87914228
374	C	-13.44553726	1.55547096	0.00196491
375	H	-13.70302454	0.94625918	0.88128339
376	H	-13.70420900	0.94528133	-0.87632779
377	C	-14.30000797	2.82952426	0.00182434
378	H	-14.04345988	3.43931684	-0.87753308
379	H	-14.04229034	3.44030374	0.88015380
380	C	-15.80965070	2.55653298	0.00297909
381	H	-16.06633871	1.94783575	0.88179890
382	H	-16.06749411	1.94680457	-0.87478728

C	-16.65554604	3.83407879	0.00278355
H	-16.44637672	4.44739458	-0.88259487
H	-17.72753839	3.60505452	0.00362778
H	-16.44520612	4.44844191	0.88715775
C	16.65554688	3.83407775	0.00236187
H	17.72753913	3.60505337	0.00328081
H	16.44639984	4.44720832	-0.88315009
H	16.44518506	4.44862597	0.88660225
O	-0.00000010	-1.23211328	-0.00293686

Optimized coordinates (Å) for Th-Thd-Th(10):

C	-1.20806377	0.50845006	-0.08189367
C	1.20806231	0.50844896	-0.08186841
C	-2.62897218	0.26196466	-0.10378363
C	-3.30724199	-0.93120312	-0.21603580
S	-3.75383772	1.60215727	0.02841576
C	-4.72047485	-0.77714338	-0.19652581
H	-2.81147972	-1.89206474	-0.30921571
C	-5.13166814	0.52795398	-0.07024494
H	-5.40815518	-1.61115399	-0.27339070
C	2.62897093	0.26196222	-0.10372872
C	3.30724201	-0.93120506	-0.21597812
S	3.75383480	1.60215297	0.02850384
C	4.72047463	-0.77714681	-0.19643585
H	2.81148083	-1.89206528	-0.30917861
C	5.13166637	0.52794882	-0.07013243
H	5.40815598	-1.61115720	-0.27329419
N	-0.67872948	1.70492656	0.03120256
N	0.67872675	1.70492594	0.03121690
C	-6.52843051	1.08964312	-0.01520250
H	-6.63703425	1.69821823	0.89371850
H	-6.67075511	1.78587795	-0.85425675
C	-7.63742108	0.02837637	-0.04680507
H	-7.54715630	-0.56880960	-0.96422752
H	-7.50229530	-0.66611570	0.79336948
C	-9.03990065	0.64625750	0.02226512
H	-9.17222518	1.34284177	-0.81852838
H	-9.12561737	1.25118318	0.93680907
C	-10.16370184	-0.39780305	-0.00177323
H	-10.07753765	-1.00321688	-0.91622769
H	-10.02923954	-1.09455842	0.83884452
C	-11.56787885	0.21628248	0.06913067
H	-11.70294970	0.91089331	-0.77327290
H	-11.65144896	0.82523051	0.98159146
C	-12.69382056	-0.82574116	0.05176856
H	-12.55817735	-1.52007882	0.89440866
H	-12.61038804	-1.43514402	-0.86048329
C	-14.09796667	-0.21162192	0.12344441
H	-14.23434321	0.48104843	-0.72048688
H	-14.18006524	0.39991695	1.03443403
C	-15.22472807	-1.25259941	0.11041363
H	-15.08953979	-1.94519598	0.95476991

H	-15.14373892	-1.86493410	-0.80029356
C	-16.62884142	-0.63855282	0.18189774
H	-16.76479738	0.05219514	-0.66254269
H	-16.70983608	-0.02632273	1.09146857
C	6.52842797	1.08963542	-0.01504594
H	6.67075337	1.78593260	-0.85404804
H	6.63702916	1.69814343	0.89392059
C	7.63741992	0.02837253	-0.04672512
H	7.54715185	-0.56875040	-0.96418831
H	7.50229921	-0.66617767	0.79340221
C	9.03989870	0.64625129	0.02238311
H	9.12562012	1.25110739	0.93697263
H	9.17221608	1.34290006	-0.81835809
C	10.16370221	-0.39780474	-0.00174333
H	10.07753458	-1.00314607	-0.91624547
H	10.02924615	-1.09462729	0.83881974
C	11.56787801	0.21627877	0.06920174
H	11.65145398	0.82514851	0.98171422
H	11.70293960	0.91096257	-0.77314316
C	12.69382278	-0.82573984	0.05173967
H	12.61038518	-1.43506245	-0.86056533
H	12.55818835	-1.52015233	0.89431953
C	14.09796741	-0.21162234	0.12345875
H	14.18007275	0.39983248	1.03450416
H	14.23433321	0.48112666	-0.72040975
C	15.22473246	-1.25259453	0.11032012
H	15.14373686	-1.86484426	-0.80044361
H	15.08955482	-1.94527067	0.95461285
C	16.62884428	-0.63854945	0.18184824
H	16.70984597	-0.02640562	1.09147650
H	16.76478881	0.05227942	-0.66252784
S	-0.00000002	-0.77125293	-0.20301612
C	17.74810507	-1.68492171	0.17003676
H	17.71426080	-2.29059304	-0.74418072
H	18.73699733	-1.21476990	0.22174887
H	17.65926346	-2.36929533	1.02298639
C	-17.74809840	-1.68493049	0.17019756
H	-18.73699188	-1.21477756	0.22187505
H	-17.71426122	-2.29068893	-0.74396246
H	-17.65924526	-2.36922236	1.02321157

Optimized coordinates (Å) for Th_3(10):

C	1.26837879	-1.21007656	0.00008198
C	0.70852443	-2.47104433	0.00033753
C	-0.70852454	-2.47104417	0.00033264
C	-1.26837862	-1.21007627	0.00007325
S	0.00000022	0.01108963	-0.00024612
H	1.30156813	-3.37954852	0.00055460
H	-1.30156847	-3.37954821	0.00053860
C	2.66280229	-0.82805285	0.00003919
C	3.22398045	0.42972758	-0.00007935
S	3.93527594	-2.04662194	0.00014213

485	C	4.64875931	0.42350348	-0.00008727
486	H	2.63410326	1.34072849	-0.00015208
487	C	5.20090459	-0.83106076	0.00002478
488	H	5.24307275	1.33020577	-0.00017238
489	C	-2.66280200	-0.82805223	0.00002622
490	C	-3.22397990	0.42972830	-0.00029443
491	S	-3.93527604	-2.04662098	0.00043851
492	C	-4.64875882	0.42350458	-0.00026313
493	H	-2.63410247	1.34072902	-0.00056956
494	C	-5.20090450	-0.83105947	0.00007857
495	H	-5.24307197	1.33020702	-0.00051052
496	C	6.64764594	-1.25032333	0.00005105
497	H	6.84287393	-1.88653100	0.87558288
498	H	6.84287901	-1.88662508	-0.87541167
499	C	-6.64764594	-1.25032175	0.00018201
500	H	-6.84289086	-1.88674621	-0.87518910
501	H	-6.84286218	-1.88640668	0.87580539
502	C	7.63992573	-0.07865094	-0.00001001
503	H	7.45912084	0.55298895	-0.88027122
504	H	7.45910740	0.55309150	0.88017475
505	C	-7.63992573	-0.07864935	-0.00002881
506	H	-7.45909269	0.55321695	0.88006408
507	H	-7.45913566	0.55286667	-0.88038190
508	C	-9.10082769	-0.54674119	0.00009762
509	H	-9.27876687	-1.18346403	-0.87896767
510	H	-9.27872242	-1.18312624	0.87941647
511	C	9.10082774	-0.54674268	0.00002772
512	H	9.27873888	-1.18324276	0.87925998
513	H	9.27875073	-1.18335047	-0.87912420
514	C	10.10788798	0.61059592	-0.00003658
515	H	9.92872375	1.24731056	-0.87907160
516	H	9.92870528	1.24742444	0.87891218
517	C	-10.10788803	0.61059728	-0.00009860
518	H	-9.92873544	1.24720246	-0.87921525
519	H	-9.92869396	1.24753527	0.87876850
520	C	-11.57042912	0.14715030	0.00002368
521	H	-11.74885435	-0.49003806	0.87900680
522	H	-11.74889954	-0.49036015	-0.87871669
523	C	11.57042906	0.14714916	0.00000916
524	H	11.74886742	-0.49014292	0.87891440
525	H	11.74888663	-0.49025751	-0.87880911
526	C	12.57923310	1.30306212	-0.00005519
527	H	12.40049099	1.94038510	-0.87892945
528	H	12.40046707	1.94050387	0.87872807
529	C	-12.57923331	1.30306307	-0.00016181
530	H	-12.40050068	1.94028629	-0.87911035
531	H	-12.40045802	1.94060463	0.87854715
532	C	-14.04195172	0.84012335	-0.00004244
533	H	-14.22049793	0.20274951	0.87889690
534	H	-14.22054301	0.20243838	-0.87874691
535	C	-15.05135891	1.99530071	-0.00022078
536	H	-14.87386773	2.63313839	-0.87918136

H	-14.87382402	2.63344742	0.87850664
C	-16.51415231	1.53281315	-0.00010308
H	-16.69196820	0.89604880	0.87832949
H	-16.69201296	0.89574338	-0.87830512
C	14.04195156	0.84012266	-0.00000369
H	14.22053285	0.20253421	-0.87878026
H	14.22050803	0.20265236	0.87886359
C	15.05135854	1.99530022	-0.00006701
H	14.87385921	2.63323209	-0.87895759
H	14.87383159	2.63335269	0.87873044
C	16.51415205	1.53281294	-0.00001206
H	16.69200450	0.89583600	-0.87828311
H	16.69197640	0.89595580	0.87835153
C	17.51529582	2.69276663	-0.00007501
H	17.38491046	3.32826236	0.88475111
H	18.54962514	2.32973201	-0.00003320
H	17.38493935	3.32814112	-0.88499243
C	-17.51529629	2.69276667	-0.00027913
H	-17.38494750	3.32804847	-0.88526422
H	-18.54962551	2.32973186	-0.00019049
H	-17.38490347	3.32835509	0.88447929

TD-DFT excitation energies and oscillator strengths for Th-Oxd-Th(10):

Excited State 1: Singlet-A 3.8397 eV 322.90 nm f = 1.1612 <S**2> = 0.000
139 ->142 0.16639
140 ->141 0.67844
This state for optimization and/or second-order correction.
Total Energy, E(TD-HF/TD-DFT) = -2151.57241331
Copying the excited state density for this state as the 1-particle RhoCI density.
Excited State 2: Singlet-A 4.7066 eV 263.42 nm f = 0.0585 <S**2> = 0.000
138 ->141 0.10602
139 ->141 0.39208
140 ->142 0.56073
Excited State 3: Singlet-A 5.1694 eV 239.84 nm f = 0.0007 <S**2> = 0.000
137 ->141 0.58692
138 ->142 -0.35150
Excited State 4: Singlet-A 5.1769 eV 239.50 nm f = 0.1757 <S**2> = 0.000
137 ->142 -0.34830
138 ->141 0.57678
139 ->141 -0.12485
Excited State 5: Singlet-A 5.3774 eV 230.57 nm f = 0.0001 <S**2>=0.000
133 ->142 0.12674
139 ->141 0.55159
140 ->142 -0.40040
Excited State 6: Singlet-A 5.6984 eV 217.58 nm f=0.0000 <S**2> = 0.000
134 ->141 0.64152
134 ->145 -0.14015
136 ->141 0.20251
Excited State 7: Singlet-A 5.9211 eV 209.39 nm f = 0.0347 <S**2> = 0.000
133 ->141 0.21742
139 ->142 0.61505
140 ->141 -0.13869

140 ->145 0.17856
Excited State 8: Singlet-A 5.9270 eV 209.19 nm f = 0.0000 <S**2> = 0.000
139 ->144 0.33420
140 ->143 0.59840
Excited State 9: Singlet-A 5.9946 eV 206.83 nm f = 0.0008 <S**2> = 0.000
139 ->143 0.37585
140 ->144 0.56656
Excited State 10: Singlet-A 6.2904 eV 197.10 nm f = 0.0067 <S**2>=0.000
116 ->141 -0.10331
118 ->141 -0.21384
122 ->141 -0.17124
134 ->142 0.54317
134 ->150 0.16147
134 ->167 -0.12540
136 ->142 0.17894
Excited State 11: Singlet-A 6.3596 eV 194.96 nm f = 0.0000 <S**2> = 0.000
137 ->143 0.48569
138 ->144 -0.45662
Excited State 12: Singlet-A 6.3618 eV 194.89 nm f = 0.0000 <S**2> = 0.000
134 ->142 -0.10948
137 ->144 -0.45141
138 ->143 0.47057
Excited State 13: Singlet-A 6.5740 eV 188.60 nm = 0.0144 <S**2> = 0.000
133 ->141 -0.16914
137 ->141 -0.30996
137 ->145 0.15244
138 ->142 -0.34737
139 ->150 -0.18597
140 ->145 0.42003
Excited State 14: Singlet-A 6.6269 eV 187.09 nm f=0.0002 <S**2>=0.000
137 ->142 0.50133
138 ->141 0.37664
138 ->145 -0.15985
139 ->145 0.15232
140 ->150 -0.19883
Excited State 15: Singlet-A 6.7394 eV 183.97 nm f=0.0251 <S**2>=0.000
137 ->141 0.20498
137 ->145 -0.10627
138 ->142 0.43762
139 ->142 -0.13396
139 ->150 -0.14540
140 ->145 0.44440
Excited State 16: Singlet-A 6.8924 eV 179.88 nm f=0.0019 <S**2>=0.000
115 ->142 0.11594
116 ->141 0.18119
118 ->141 0.40486
122 ->141 0.36915
134 ->142 0.28832
135 ->141 -0.10094
Excited State 17: Singlet-A 6.9960 eV 177.22 nm f = 0.3755 S**2>=0.000
113 ->141 -0.14081
137 ->142 0.28490

```
640          139 ->145         -0.28752
641          140 ->150          0.52557
642     Excited State  18:      Singlet-A      7.0016 eV  177.08 nm  f=0.0091  <S**2>=0.000
643          133 ->141          0.60542
644          138 ->142         -0.11100
645          139 ->142         -0.23165
646          140 ->141          0.10649
647     Excited State  19:      Singlet-A      7.0156 eV  176.73 nm  f=0.0000  <S**2>=0.000
648          110 ->142          0.10494
649          112 ->141         -0.10370
650          114 ->142          0.20899
651          115 ->141          0.36301
652          117 ->141          0.10405
653          121 ->141          0.31625
654          122 ->142          0.28720
655          135 ->142         -0.14145
656          136 ->141         -0.21074
657     Excited State  20:      Singlet-A      7.0690 eV  175.39 nm  f=0.0085  <S**2>=0.000
658          110 ->141          0.17679
659          114 ->141          0.37381
660          115 ->142          0.24180
661          116 ->141         -0.19952
662          118 ->141         -0.19438
663          121 ->142          0.21296
664          122 ->141          0.18842
665          122 ->145          0.10014
666          135 ->141         -0.21212
667          136 ->142         -0.14511
668     Excited State  21:      Singlet-A      7.0864 eV  174.96 nm  f=0.0000  <S**2>=0.000
669          139 ->144         -0.16326
670          140 ->147         -0.13963
671          140 ->149          0.13149
672          140 ->152         -0.21062
673          140 ->153          0.29669
674          140 ->154          0.32012
675          140 ->159         -0.27770
676          140 ->162         -0.23557
677     Excited State 22:       Singlet-A      7.3232 eV  169.30 nm  f=0.0000  <S**2>=0.000
678          139 ->147         -0.18742
679          139 ->149          0.16438
680          139 ->152         -0.14061
681          140 ->144         -0.12821
682          140 ->146          0.34304
683          140 ->148         -0.28060
684          140 ->151          0.21270
685          140 ->161         -0.16377
686          140 ->163          0.13354
687          140 ->169         -0.11490
688          140 ->170          0.15360
689     Excited State  23:      Singlet-A      7.4056 eV  167.42 nm  f=0.0000  <S**2>=0.000
690          139 ->144          0.14018
691          139 ->158          0.11313
```

139 ->163 -0.19155
140 ->153 0.50296
140 ->159 0.18105
140 ->162 0.22337
140 ->168 0.12670
Excited State 24: Singlet-A 7.4385 eV 166.68 nm f=0.0000 <S**2>=0.000
136 ->141 0.11977
139 ->146 -0.19282
139 ->148 0.16348
139 ->151 -0.13568
140 ->147 0.33618
140 ->149 -0.26475
140 ->152 0.16583
140 ->153 0.11341
140 ->154 0.10884
140 ->159 -0.11322
140 ->160 -0.15120
140 ->162 -0.14973
140 ->168 -0.11390
Excited State 25: Singlet-A 7.4553 eV 166.30 nm f=0.0009 <S**2>=0.000
139 ->143 0.16129
139 ->153 -0.11429
139 ->154 0.10306
139 ->159 -0.15927
139 ->162 -0.17987
139 ->168 -0.11816
140 ->146 -0.15137
140 ->148 0.12997
140 ->151 -0.13059
140 ->155 0.15112
140 ->158 -0.26395
140 ->163 0.37400
140 ->170 0.15430
Excited State 26: Singlet-A 7.5037 eV 165.23 nm f=0.0000 <S**2>=0.000
104 ->142 -0.13497
105 ->141 0.13491
107 ->141 0.17020
110 ->142 0.14865
112 ->141 -0.20770
114 ->142 0.13178
115 ->141 0.29385
121 ->141 -0.12739
134 ->141 -0.11645
135 ->142 0.15633
136 ->141 0.33751
140 ->147 -0.12163
140 ->153 -0.11847
Excited State 27: Singlet-A 7.5451 eV 164.32 nm f=0.0224 <S**2>=0.000
108 ->141 -0.13687
111 ->141 0.18370
113 ->141 0.16512
133 ->142 0.44961

744 137 ->150 0.21846
745 138 ->145 0.23926
746 139 ->141 -0.10379
747 140 ->167 0.18617
748 Excited State 28: Singlet-A 7.5572 eV 164.06 nm f=0.0000 <S**2>=0.000
749 114 ->142 -0.21459
750 116 ->142 0.25632
751 118 ->142 0.45963
752 118 ->150 0.13839
753 118 ->167 -0.10476
754 122 ->142 0.25208
755 Excited State 29: Singlet-A 7.5636 eV 163.92 nm f=0.0011 <S**2>=0.000
756 104 ->141 -0.20068
757 105 ->142 0.10349
758 107 ->142 0.12348
759 110 ->141 0.24180
760 112 ->142 -0.15071
761 114 ->141 0.23230
762 115 ->142 0.21505
763 118 ->141 0.11659
764 135 ->141 0.37713
765 136 ->142 0.17981
766 Excited State 30: Singlet-A 7.6332 eV 162.43 nm f=0.2315 <S**2>=0.000
767 137 ->145 0.46672
768 138 ->142 0.18205
769 138 ->150 0.40275
770 139 ->150 -0.12803
771 140 ->166 -0.13622

772 **TD-DFT excitation energies and oscillator strengths for Th-Thd-Th(10):**

773 Excited State 1: Singlet-A 3.5070 eV 353.53 nm f=1.1804 <S**2>=0.000
774 143 ->146 0.13462
775 144 ->145 0.68560
776 This state for optimization and/or second-order correction.
777 Total Energy, E(TD-HF/TD-DFT) = -2474.55713381
778 Copying the excited state density for this state as the 1-particle RhoCI density.
779 Excited State 2: Singlet-A 4.4743 eV 277.10 nm f=0.0001 <S**2>=0.000
780 143 ->145 0.54962
781 144 ->146 0.41215
782 Excited State 3: Singlet-A 4.7187 eV 262.75 nm f=0.0000 <S**2>=0.000
783 140 ->145 0.68229
784 140 ->148 0.13663
785 Excited State 4: Singlet-A 4.9413 eV 250.92 nm f=0.0964 <S**2>=0.000
786 141 ->146 -0.27999
787 142 ->145 0.60751
788 143 ->145 0.16448
789 Excited State 5: Singlet-A 4.9658 eV 249.67 nm f=0.0061 <S**2>=0.000
790 141 ->145 0.62700
791 142 ->146 -0.28821
792 Excited State 6: Singlet-A 5.1295 eV 241.71 nm f=0.0139 <S**2>=0.000
793 142 ->145 0.14946
794 143 ->145 -0.38413

143 ->148 -0.12713
144 ->146 0.53809
Excited State 7: Singlet-A 5.3658 eV 231.06 nm f=0.0006 <S**2>=0.000
136 ->147 -0.13272
144 ->147 0.67553
Excited State 8: Singlet-A 5.6407 eV 219.80 nm f=0.0013 <S**2>=0.000
133 ->145 0.52447
140 ->146 -0.40254
140 ->155 -0.12979
144 ->147 -0.10696
Excited State 9: Singlet-A 5.7387 eV 216.05 nm f=0.1112 <S**2>=0.000
136 ->145 0.21706
143 ->146 0.58147
144 ->148 -0.28253
Excited State 10: Singlet-A 5.8126 eV 213.30 nm f=0.0303 <S**2>=0.000
136 ->146 -0.10062
137 ->145 0.64223
140 ->147 0.16350
Excited State 11: Singlet-A 5.8558 eV 211.73 nm f=0.0002 <S**2>=0.000
143 ->147 -0.18070
143 ->150 0.26175
144 ->149 0.59726
Excited State 12: Singlet-A 6.0214 eV 205.91 nm f=0.0011 <S**2>=0.000
133 ->145 -0.14580
140 ->146 -0.11898
143 ->149 0.36392
144 ->150 0.50896
144 ->152 -0.15647
Excited State 13: Singlet-A 6.1099 eV 202.92 nm f=0.0038 <S**2>=0.000
133 ->145 0.39510
140 ->146 0.49361
140 ->155 0.14768
143 ->149 0.10918
144 ->150 0.14781
Excited State 14: Singlet-A 6.1768 eV 200.73 nm f=0.0000 <S**2>=0.000
137 ->147 0.38238
142 ->147 0.10202
143 ->147 0.53709
143 ->150 0.10905
144 ->149 0.13514
Excited State 15: Singlet-A 6.3335 eV 195.76 nm f=0.0067 <S**2>=0.000
136 ->145 0.30318
141 ->145 -0.20038
141 ->148 -0.16839
142 ->146 -0.28521
143 ->155 0.18149
144 ->148 0.43790
Excited State 16: Singlet-A 6.3823 eV 194.26 nm f=0.0002 <S**2>=0.000
141 ->147 0.15331
141 ->150 -0.40636
141 ->152 0.12986
142 ->149 0.47299

Excited State	17:	Singlet-A	6.3871 eV	194.12 nm	f=0.0000	<S**2>=0.000
141 ->149		0.47975				
142 ->147		0.13512				
142 ->150		-0.39778				
142 ->152		0.12746				
143 ->150		-0.10594				
Excited State	18:	Singlet-A	6.4570 eV	192.01 nm	f=0.0031	<S**2>=0.000
137 ->145		-0.10085				
141 ->146		0.50008				
142 ->145		0.30150				
142 ->148		0.21920				
143 ->148		0.17744				
144 ->155		0.19138				
Excited State	19:	Singlet-A	6.5242 eV	190.04 nm	f=0.0757	<S**2>=0.000
141 ->145		0.20347				
141 ->148		0.17401				
142 ->146		0.44590				
143 ->146		0.20349				
144 ->148		0.37967				
Excited State	20:	Singlet-A	6.6944 eV	185.21 nm	f=0.0010	<S**2>=0.000
136 ->145		0.55620				
137 ->146		-0.11522				
141 ->145		0.10055				
142 ->146		0.20532				
143 ->146		-0.24397				
144 ->145		0.11098				
144 ->148		-0.10053				
Excited State	21:	Singlet-A	6.8314 eV	181.49 nm	f=0.2001	<S**2>=0.000
140 ->147		-0.27549				
141 ->146		-0.26409				
143 ->148		0.29197				
144 ->153		-0.12434				
144 ->155		0.43394				
Excited State	22:	Singlet-A	6.8374 eV	181.33 nm	f=0.0000	<S**2>=0.000
117 ->146		-0.15989				
118 ->145		0.37991				
123 ->146		0.13395				
124 ->145		0.27591				
133 ->146		0.36296				
139 ->145		-0.17930				
Excited State	23:	Singlet-A	6.9028 eV	179.61 nm	f=0.0064	<S**2>=0.000
114 ->145		-0.14222				
117 ->145		-0.33787				
118 ->146		0.23649				
119 ->145		0.12307				
123 ->145		0.34030				
124 ->146		0.21139				
138 ->145		-0.26525				
139 ->146		-0.12211				
Excited State	24:	Singlet-A	6.9601 eV	178.14 nm	f=0.0000	<S**2>=0.000
137 ->147		-0.12830				
143 ->150		0.22079				

143 ->178 -0.11140
144 ->156 0.14121
144 ->158 0.47414
144 ->163 -0.18195
144 ->169 0.20726
Excited State 25: Singlet-A 7.0702 eV 175.36 nm f=0.0000 <S**2>=0.000
111 ->145 -0.13921
117 ->146 0.10414
123 ->146 -0.17663
124 ->145 -0.21380
133 ->146 0.44611
133 ->155 0.15483
139 ->145 0.27099
144 ->158 -0.12091
Excited State 26: Singlet-A 7.1966 eV 172.28 nm f=0.0000 <S**2>=0.000
118 ->145 -0.12226
137 ->147 -0.48892
139 ->145 -0.11810
143 ->147 0.32931
144 ->158 -0.19148
144 ->159 -0.10344
Excited State 27: Singlet-A 7.2334 eV 171.41 nm f=0.0000 <S**2>=0.000
110 ->146 -0.10281
111 ->145 -0.20097
114 ->146 -0.13037
115 ->145 -0.16591
117 ->146 -0.17092
118 ->145 0.35564
133 ->146 -0.26648
133 ->155 -0.10352
137 ->147 -0.15400
139 ->145 0.26259
143 ->147 0.11741
Excited State 28: Singlet-A 7.2689 eV 170.57 nm f=0.0132 <S**2>=0.000
133 ->147 -0.12287
137 ->146 0.62523
137 ->155 0.12744
143 ->146 -0.11783
144 ->148 -0.10865
Excited State 29: Singlet-A 7.2892 eV 170.09 nm f=0.0107 <S**2>=0.000
140 ->147 -0.12446
143 ->151 0.18465
143 ->154 -0.16801
143 ->156 0.14777
143 ->165 0.10297
144 ->150 0.20034
144 ->152 0.30387
144 ->153 0.28802
144 ->157 -0.21871
144 ->166 0.15341
Excited State 30: Singlet-A 7.3187 eV 169.41 nm f=0.0002 <S**2>=0.000
143 ->152 0.18274

143 ->153 0.16843
143 ->157 -0.14315
144 ->151 0.34681
144 ->154 -0.29297
144 ->156 0.21631
144 ->163 0.14280
144 ->165 0.15538
144 ->169 -0.18547

TD-DFT excitation energies and oscillator strengths for Th_3(10):

Excited State 1: Singlet-A 3.2352 eV 383.23 nm f=1.1501 <S**2>=0.000
143 ->146 0.10496
144 ->145 0.69331
This state for optimization and/or second-order correction.
Total Energy, E(TD-HF/TD-DFT) = -2442.48397494
Copying the excited state density for this state as the 1-particle RhoCI density.
Excited State 2: Singlet-A 4.4727 eV 277.20 nm f=0.0114 <S**2>=0.000
140 ->145 -0.13771
143 ->145 0.41305
144 ->146 0.53540
Excited State 3: Singlet-A 4.9600 eV 249.97 nm f=0.0009 <S**2>=0.000
139 ->146 -0.12084
140 ->145 0.12421
142 ->145 0.24007
143 ->145 0.52412
144 ->146 -0.33903
Excited State 4: Singlet-A 5.0025 eV 247.84 nm f=0.0001 <S**2>=0.000
140 ->145 0.18829
141 ->146 -0.15922
142 ->145 0.57887
143 ->145 -0.17322
144 ->146 0.24500
Excited State 5: Singlet-A 5.1535 eV 240.58 nm f=0.0025 <S**2>=0.000
140 ->146 0.11974
141 ->145 0.61946
142 ->146 -0.24148
144 ->149 0.12542
Excited State 6: Singlet-A 5.2003 eV 238.42 nm f=0.0002 <S**2>=0.000
139 ->148 0.11993
144 ->148 0.65392
144 ->150 0.20644
Excited State 7: Singlet-A 5.2659 eV 235.45 nm f=0.2023 <S**2>=0.000
140 ->145 0.59885
141 ->146 0.21978
142 ->145 -0.17621
143 ->149 0.10311
144 ->146 0.11921
144 ->157 -0.12382
Excited State 8: Singlet-A 5.3190 eV 233.10 nm f=0.0000 <S**2>=0.000
143 ->150 -0.22838
144 ->147 0.63700
Excited State 9: Singlet-A 5.4861 eV 226.00 nm f=0.0009 <S**2>=0.000

143 ->147 -0.30436
144 ->148 -0.19118
144 ->150 0.56937
Excited State 10: Singlet-A 5.7371 eV 216.11 nm f=0.0898 <S**2>=0.000
139 ->145 -0.19445
141 ->145 -0.14198
143 ->146 0.38087
144 ->149 0.51601
Excited State 11: Singlet-A 6.0924 eV 203.51 nm f=0.0080 <S**2>=0.000
139 ->145 0.51640
140 ->146 0.11207
143 ->146 -0.24081
143 ->157 -0.10360
144 ->149 0.35163
Excited State 12: Singlet-A 6.2170 eV 199.43 nm f=0.0000 <S**2>=0.000
140 ->148 0.43473
140 ->150 0.17204
142 ->148 0.35622
143 ->148 -0.32545
Excited State 13: Singlet-A 6.2258 eV 199.15 nm f=0.0001 <S**2>=0.000
140 ->147 -0.21337
141 ->148 -0.15016
141 ->150 0.42272
142 ->147 0.41946
143 ->147 -0.14830
Excited State 14: Singlet-A 6.2301 eV 199.01 nm f=0.0000 <S**2>=0.000
140 ->148 0.16562
140 ->150 -0.16123
141 ->147 0.47248
142 ->150 0.38420
143 ->150 -0.12741
Excited State 15: Singlet-A 6.3848 eV 194.19 nm f=0.0000 <S**2>=0.000
139 ->147 0.10077
143 ->150 0.20691
144 ->158 0.12446
144 ->160 -0.29750
144 ->162 0.52143
144 ->166 -0.10013
144 ->173 -0.10046
Excited State 16: Singlet-A 6.5583 eV 189.05 nm f=0.0785 <S**2>=0.000
139 ->145 -0.21790
140 ->146 0.22034
141 ->145 0.17733
141 ->149 -0.15636
142 ->146 0.47097
143 ->146 -0.28815
144 ->149 0.13947
Excited State 17: Singlet-A 6.5981 eV 187.91 nm f=0.0572 <S**2>=0.000
140 ->145 0.22905
141 ->146 -0.35047
142 ->145 -0.20032
142 ->149 0.18471

143 ->149 -0.25489
144 ->157 0.35732
144 ->163 0.12281
Excited State 18: Singlet-A 6.7410 eV 183.93 nm f=0.0047 <S**2>=0.000
121 ->146 -0.15110
124 ->145 -0.43713
126 ->145 0.48565
Excited State 19: Singlet-A 6.7490 eV 183.71 nm f=0.0404 <S**2>=0.000
139 ->145 0.32421
140 ->146 0.17189
142 ->146 0.32710
143 ->146 0.41507
144 ->145 -0.11702
144 ->149 -0.18198
Excited State 20: Singlet-A 6.7642 eV 183.29 nm f=0.0000 <S**2>=0.000
140 ->148 0.10227
143 ->148 0.12138
143 ->168 -0.10086
144 ->151 0.14359
144 ->153 -0.14284
144 ->156 0.16845
144 ->160 0.50528
144 ->162 0.26350
Excited State 21: Singlet-A 6.8325 eV 181.46 nm f=0.0029 <S**2>=0.000
139 ->145 -0.12983
140 ->146 0.55172
141 ->145 -0.19479
141 ->149 0.24496
142 ->146 -0.10988
144 ->169 0.10752
144 ->172 0.12705
Excited State 22: Singlet-A 6.8371 eV 181.34 nm f=0.0005 <S**2>=0.000
143 ->151 0.15153
143 ->153 -0.14615
143 ->156 0.12087
144 ->150 -0.12148
144 ->152 0.39264
144 ->154 -0.35542
144 ->155 0.26005
144 ->164 0.14586
Excited State 23: Singlet-A 6.8658 eV 180.58 nm f=0.0000 <S**2>=0.000
143 ->152 0.13304
143 ->154 -0.13296
143 ->155 0.10352
144 ->151 0.37744
144 ->153 -0.31825
144 ->156 0.19876
144 ->160 -0.23391
144 ->166 0.17936
144 ->175 0.12662
Excited State 24: Singlet-A 6.9527 eV 178.33 nm f=0.5434 <S**2>=0.000
140 ->149 0.13155

141 ->146		0.40916					
142 ->145		0.13324					
142 ->149		-0.18033					
143 ->149		-0.18570					
144 ->157		0.40079					
144 ->163		0.11667					
144 ->170		-0.13318					
144 ->171		0.11015					
Excited State	25:	Singlet-A	6.9796 eV	177.64 nm	f=0.0000	<S**2>=0.000	
121 ->145		0.51090					
125 ->145		0.32714					
126 ->146		-0.25877					
Excited State	26:	Singlet-A	7.0175 eV	176.68 nm	f=0.0009	<S**2>=0.000	
139 ->148		0.10075					
143 ->147		-0.17571					
143 ->158		-0.12106					
143 ->162		-0.22564					
144 ->150		-0.13309					
144 ->159		-0.10324					
144 ->164		-0.28123					
144 ->168		0.44776					
Excited State	27:	Singlet-A	7.1144 eV	174.27 nm	f=0.0000	<S**2>=0.000	
140 ->148		0.24262					
142 ->148		0.10358					
143 ->148		0.45693					
143 ->150		0.21545					
144 ->162		-0.23352					
144 ->165		0.16471					
144 ->173		-0.14445					
Excited State	28:	Singlet-A	7.1596 eV	173.17 nm	f=0.0020	<S**2>=0.000	
114 ->145		-0.17717					
118 ->145		-0.28277					
119 ->145		0.10392					
121 ->146		0.11144					
124 ->145		-0.26405					
125 ->146		0.23664					
126 ->145		-0.26854					
126 ->149		-0.11796					
137 ->145		0.28692					
138 ->146		-0.12358					
Excited State	29:	Singlet-A	7.2077 eV	172.02 nm	f=0.0083	<S**2>=0.000	
139 ->146		-0.13113					
141 ->146		0.12497					
143 ->169		-0.11253					
143 ->172		-0.13142					
144 ->157		0.16827					
144 ->170		0.57395					
144 ->171		-0.19441					
Excited State	30:	Singlet-A	7.2624 eV	170.72 nm	f=0.0000	<S**2>=0.000	
112 ->145		0.25008					
116 ->145		0.13405					
120 ->145		-0.10514					

121	->145	0.23442
124	->146	0.14355
125	->145	-0.25429
137	->146	-0.13388
138	->145	0.35980
143	->148	-0.12958

References

1. Lavigueur, C.; Foster, E.J.; Williams, V.E. A simple and inexpensive capillary furnace for variable-temperature X-ray diffraction. *J. Appl. Crystallogr.* **2008**, *41*, 214–216.
2. Boucher, N.; Leroy, J.; Sergeyev, S.; Pouzet, E.; Lemaur, V.; Lazzaroni, R.; Cornil, J.; Geerts, Y.H.; Sferrazza, M. Mesomorphism of dialkylterthiophene homologues. *Synth. Met.* **2009**, *159*, 1319–1324.
3. Bruker, APEX3, SAINT and SADABS, Bruker AXS Inc., Madison, Wisconsin, USA, 2016.
4. G. M. Sheldrick, TWINABS (Version 2012/1), University of Gçttingen, Germany, 1996.
5. Sheldrick, G.M. Crystal structure refinement with SHELXL. *Acta Crystallogr. Sect. C Struct. Chem.* **2015**, *71*, 3–8.
6. Hübschle, C.B.; Sheldrick, G.M.; Dittrich, B. ShelXle: a Qt graphical user interface for SHELXL. *J. Appl. Crystallogr.* **2011**, *44*, 1281–1284.
7. Farrugia, L.J. WinGX and ORTEP for Windows: an update. *J. Appl. Crystallogr.* **2012**, *45*, 849–854.
8. Fenn, T.D.; Ringe, D.; Petsko, G.A. POVScript+: a program for model and data visualization using persistence of vision ray-tracing. *J. Appl. Crystallogr.* **2003**, *36*, 944–947.
9. Lercher, C.; Röthel, C.; Roscioni, O.M.; Geerts, Y.H.; Shen, Q.; Teichert, C.; Fischer, R.; Leising, G.; Sferrazza, M.; Gbabode, G.; et al. Polymorphism of dioctyl-terthiophene within thin films: The role of the first monolayer. *Chem. Phys. Lett.* **2015**, *630*, 12–17.
10. Van Bolhuis, F.; Wynberg, H.; Havinga, E.E.; Meijer, E.W.; Staring, E.G.J. The X-ray structure and MNDO calculations of α-terthienyl: A model for polythiophenes. *Synth. Met.* **1989**, *30*, 381–389.
11. Resch-Genger, U.; Rurack, K. Determination of the photoluminescence quantum yield of dilute dye solutions (IUPAC Technical Report). *Pure Appl. Chem.* **2013**, *85*, 2005–2013.
12. Brouwer, A.M. Standards for photoluminescence quantum yield measurements in solution (IUPAC Technical Report). *Pure Appl. Chem.* **2011**, *83*, 2213–2228.
13. Stephens, P.J.; Devlin, F.J.; Chabalowski, C.F.; Frisch, M.J. Ab Initio Calculation of Vibrational Absorption and Circular Dichroism Spectra Using Density Functional Force Fields. *J. Phys. Chem.* **1994**, *98*, 11623–11627.
14. Becke, A.D. Density-functional thermochemistry. III. The role of exact exchange. *J. Chem. Phys.* **1993**, *98*, 5648–5652.
15. Tomasi, J.; Mennucci, B.; Cancès, E. The IEF version of the PCM solvation method: an overview of a new method addressed to study molecular solutes at the QM ab initio level. *J. Mol. Struct. THEOCHEM* **1999**, *464*, 211–226.
16. Barone, V.; Cossi, M.; Tomasi, J. Geometry optimization of molecular structures in solution by the polarizable continuum model. *J. Comput. Chem.* **1998**, *19*, 404–417.
17. Barone, V.; Cossi, M.; Tomasi, J. A new definition of cavities for the computation of solvation free energies by the polarizable continuum model. *J. Chem. Phys.* **1997**, *107*, 3210–3221.
18. Miertuš, S.; Scrocco, E.; Tomasi, J. Electrostatic interaction of a solute with a continuum. A direct utilizaion of AB initio molecular potentials for the prevision of solvent effects. *Chem. Phys.* **1981**, *55*, 117–129.
19. Gaussian 16, Revision B.01, M. J. Frisch, G. W. Trucks, H. B. Schlegel, G. E. Scuseria, M. A. Robb, J. R. Cheeseman, G. Scalmani, V. Barone, G. A. Petersson, H. Nakatsuji, X. Li, M. Caricato, A. V. Marenich, J. Bloino, B. G. Janesko, R. Gomperts, B. Mennucci, H. P. Hratchian, J. V. Ortiz, A. F. Izmaylov, J. L. Sonnenberg, D. Williams-Young, F. Ding, F. Lipparini, F. Egidi, J. Goings, B. Peng, A. Petrone, T. Henderson, D. Ranasinghe, V. G. Zakrzewski, J. Gao, N. Rega, G. Zheng, W. Liang, M. Hada, M. Ehara, K. Toyota, R. Fukuda, J. Hasegawa, M. Ishida, T. Nakajima, Y. Honda, O. Kitao, H. Nakai, T. Vreven, K. Throssell, J. A. Montgomery, Jr., J. E. Peralta, F. Ogliaro, M. J. Bearpark, J. J. Heyd, E. N. Brothers, K. N. Kudin, V. N. Staroverov, T. A. Keith, R. Kobayashi, J. Normand, K. Raghavachari, A. P. Rendell, J. C. Burant, S. S. Iyengar, J. Tomasi, M. Cossi, J. M. Millam, M. Klene, C. Adamo, R. Cammi, J. W. Ochterski, R. L. Martin, K. Morokuma, O. Farkas, J. B. Foresman, and D. J. Fox, Gaussian, Inc., Wallingford CT, 2016.

20. Schäfer, A.; Huber, C.; Ahlrichs, R. Fully optimized contracted Gaussian basis sets of triple zeta valence quality for atoms Li to Kr. *J. Chem. Phys.* **1994**, *100*, 5829–5835.
21. Schäfer, A.; Horn, H.; Ahlrichs, R. Fully optimized contracted Gaussian basis sets for atoms Li to Kr. *J. Chem. Phys.* **1992**, *97*, 2571–2577.
22. Stratmann, R.E.; Scuseria, G.E.; Frisch, M.J. An efficient implementation of time-dependent density-functional theory for the calculation of excitation energies of large molecules. *J. Chem. Phys.* **1998**, *109*, 8218–8224.
23. Casida, M.E. Time-Dependent Density Functional Response Theory for Molecules. In *Recent Advances in Density Functional Methods*; Recent Advances in Computational Chemistry; WORLD SCIENTIFIC, 1995; Vol. Volume 1, pp. 155–192 ISBN 978-981-02-2442-4.
24. Huff, G.S.; Gallaher, J.K.; Hodgkiss, J.M.; Gordon, K.C. No single DFT method can predict Raman cross-sections, frequencies and electronic absorption maxima of oligothiophenes. *Synth. Met.* **2017**, *231*, 1–6.
25. Jacquemin, D.; Michaux, C.; Perpète, E.A.; Maurel, F.; Perrier, A. Photochromic molecular wires: Insights from theory. *Chem. Phys. Lett.* **2010**, *488*, 193–197.
26. Yanai, T.; Tew, D.P.; Handy, N.C. A new hybrid exchange–correlation functional using the Coulomb-attenuating method (CAM-B3LYP). *Chem. Phys. Lett.* **2004**, *393*, 51–57.